



PERGAMON

Deep-Sea Research II 49 (2002) 2377–2402

DEEP-SEA RESEARCH  
PART II

www.elsevier.com/locate/dsr2

# Distribution, annual cycle, and vertical migration of acoustically derived biomass in the Arabian Sea during 1994–1995

Carin J. Ashjian<sup>a,\*</sup>, Sharon L. Smith<sup>b</sup>, Charles N. Flagg<sup>c</sup>, Nasseer Idrisi<sup>b</sup>

<sup>a</sup> *Department of Biology, Woods Hole Oceanographic Institution, Woods Hole, MA 02543, USA*

<sup>b</sup> *Rosenstiel School of Marine and Atmospheric Sciences, University of Miami, 4600 Rickenbacker Causeway, Miami, FL 33149, USA*

<sup>c</sup> *Department of Applied Science, Brookhaven National Laboratory, Upton, NY 11973, USA*

Received 10 April 2001; received in revised form 1 November 2001; accepted 2 December 2001

## Abstract

The distinguishing characteristic that sets the Arabian Sea apart from other oceanic regions is the regular oscillation of monsoonal atmospheric conditions that produces predictable periods of upwelling or convective mixing, with associated biological response, during the Southwest and Northeast monsoons, respectively. This oscillation is also evident in cycles of standing stocks of zooplankton and micronekton. The vertical distribution and spatial pattern of zooplankton and micronekton biomass were estimated using an acoustic Doppler current profiler along a 1000-km transect extending from the continental shelf of Oman to the central Arabian Sea during ten cruises on the R/V *Thomas G. Thompson* (November 1994–December 1995). The influence of the Southwest Monsoon, and accompanying upwelling and enhanced acoustically derived biomass, was the dominant feature in the spatial-temporal distributions of both zooplankton and micronekton near the Omani coast. The diel vertical migration of predators (myctophids, pelagic crabs), and the seasonal changes in the strength of this signal, was the most significant pattern observed in the vertical distribution of biomass and imparted a strong day–night signal to the integrated upper water-column biomass. Significant differences in the magnitude of integrated upper water-column biomass, both zooplankton (day) and migrator-zooplankton (night), were seen between inshore and offshore of the atmospheric Findlater Jet. A station located in the central Arabian Sea demonstrated seasonal changes in biomass over the year, despite being quite far from the influence of the monsoonal oscillations. Predation pressure was greater offshore of the Findlater Jet than in the region inshore of the Jet or in the central Arabian Sea. The pelagic community of the Arabian Sea may have evolved life history strategies to coincide with the predictable monsoonal cycle. © 2002 Elsevier Science Ltd. All rights reserved.

## 1. Introduction

Seasonal cycles in abundance and distribution of zooplankton and micronekton in the northern Arabian Sea are influenced profoundly by the

ocean's response to oscillating monsoon winds. The Arabian Sea is characterized by a regular, seasonal monsoon cycle consisting of the Northeast Monsoon (NEM: December–February; prevailing winds from the NE), and the Southwest Monsoon (SWM: June–September; strong, prevailing winds from the SW, centered on the tropospheric Findlater Jet which runs SW:NE well

\*Corresponding author.

E-mail address: cashjian@whoi.edu (C.J. Ashjian).

offshore of the coast of Oman), punctuated by Intermonsoon periods (e.g., Currie et al., 1973; Schott et al., 1990; Morrison et al., 1998). The prevailing winds have dramatic effects on the hydrographic and advective fields of the region, with attendant influences on biological processes and distributions. During the SWM, upwelling of nutrient-rich water off Oman promotes primary, and hence secondary, production (e.g., Banse, 1987; Brock et al., 1991, 1992; Brock and McClain, 1992). The offshore (100–400 km) and alongshore (>1000 km) extent of relatively cool sea surface temperatures (<26°C; or approximately 4°C cooler than the adjacent sea surface not affected by upwelling) make this one of the largest upwelling areas known. Only the upwelling areas associated with the Benguela Current System (Lutjeharms and Stockton, 1987) have dimensions similar to the one off of Oman; all other upwelling regions (Peru, 1983; Somalia, Brown et al., 1980; northwest Africa, Estrada, 1974) are less extensive. The situation is different during the NEM, when cool, dry winds from the northeast cause convective mixing and associated primary productivity (Marra et al., 1998; Madhupratap et al., 1998; Barber et al., 2001). The two monsoonal regimes are separated by Spring and Fall Intermonsoon periods, characterized by a reduction of wind stress over the ocean surface and consequential diminishing of the upper mixed-layer depth (Gardner et al., 1999). As a result, primary production and phytoplankton standing crop are minimal during the Spring Intermonsoon (Gunderson et al., 1998; Marra et al., 1998; Caron and Dennett, 1999; Gardner et al., 1999). This annual oscillation should be evident in cycles of standing stock of zooplankton and micronekton, especially in the upwelling region within 600 km of the Omani coast (Smith et al., 1998b; Wishner et al., 1998).

The SWM, and its associated upwelling and enhanced primary production, is accompanied by an elevation in zooplankton biomass (e.g., Qasim, 1977; Smith and Codispoti, 1980; Smith, 1982, 1984; Matthew et al., 1990; Baars and Oosterhuis, 1997; Brink et al., 1998; Smith et al., 1998a; Wishner et al., 1998). Another pattern observed during the SWM is a pronounced

onshore–offshore declining gradient in mesozooplankton biomass (e.g., Qasim, 1977; Smith et al., 1998b; Wishner et al., 1998). The community composition of the zooplankton also may be modified during the SWM; some copepod species (e.g., *Calanoides carinatus*) increased in abundance in greater proportions than other species (e.g., Smith, 1982; Smith et al., 1998b).

The influence of the monsoonal oscillation on hydrographic and advective structure, the attendant changes in plankton and fish biomass, production, community structure, and the utilization and cycling of carbon, were addressed during the multidisciplinary Arabian Sea Expedition of 1994–1996 under the joint auspices of the US Joint Global Ocean Flux Study (JGOFS; National Science Foundation) and the Forced Upper Ocean Dynamics Project (Office of Naval Research). During the study period, a series of ten cruises were conducted on the R/V *Thomas G. Thompson* in the northern and central Arabian Sea over a full year, spanning the complete monsoon cycle. The *Thompson* was equipped with a 153 kHz RDI acoustic Doppler current profiler, which operated continuously throughout all of the cruises. The present study utilizes the backscatter intensity data collected by this instrument to analyze spatial and seasonal patterns in zooplankton and micronekton biomass across a 1000-km transect of the Arabian Sea. The transect was situated so that the atmospheric Findlater Jet (SWM) crossed the center (Fig. 1) so that the transect surveyed regions both inshore and offshore of the loci of strongest SWM winds. The abundance and distribution patterns documented by the ADCP span an entire year and were obtained continuously across the transect, in contrast to the net-based sampling, which was limited to a smaller subset of the cruises and occurred at discrete locations (Smith et al., 1998b; Wishner et al., 1998). Hence, the ADCP data describe the temporal and spatial patterns with greater temporal and spatial resolution than possible from the net-based sampling and complement the results of those studies.

Acoustic Doppler current profilers (ADCPs) have been used to describe the spatial and temporal patterns in the distribution of zooplankton biomass in many oceanic regions and

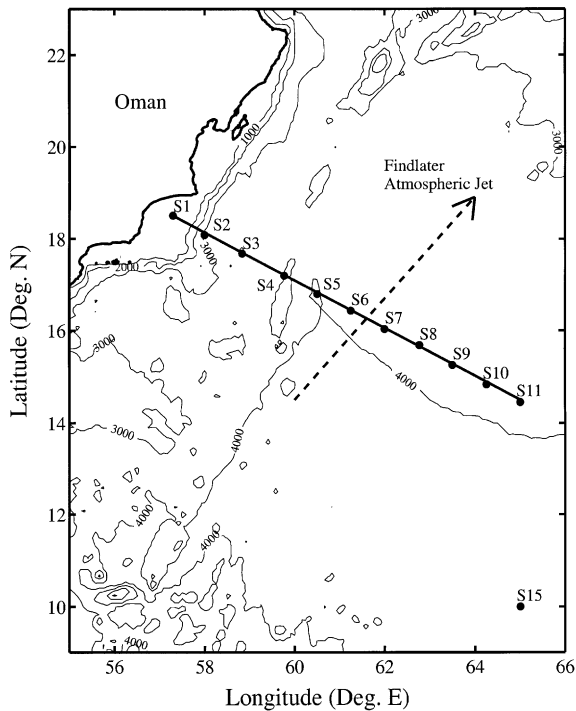


Fig. 1. Location of transect in the northern Arabian Sea. Distances along the transect are calculated as distance offshore. Standard stations (S1–S11, S15) for the US JGOFS Process study cruises (Smith et al., 1998a) are shown. The approximate location of the atmospheric Findlater Jet relative to the transect and standard stations is demonstrated. Seasonal upwelling occurs inshore of the Findlater Jet (S2–S4) during the SW Monsoon.

environments (Flagg and Smith, 1989; Plueddemann and Pinkel, 1989; Heywood et al., 1991; Smith et al., 1992; Fischer and Visbeck, 1993; Roe and Griffiths, 1993; Ashjian et al., 1994; Flagg et al., 1994; Lyons et al., 1994; Zhou et al., 1994; Batchelder et al., 1995; Buchholz et al., 1995; Heywood, 1996; Ashjian et al., 1998; Luo et al., 2000). In such studies, backscatter intensity routinely is converted to equivalent zooplankton biomass using a biomass-intensity regression derived from net-collected zooplankton samples and spatially and temporally coincident acoustic backscatter intensities. Such a relationship provides only a rough estimate of the potential biomass in the water column, since it assumes that the total backscatter intensity is derived from

scattering off of the organisms collected in the net tows. In reality, organisms that are not collected quantitatively in zooplankton net tows, such as fish, fast swimming euphausiids, and siphonophores, also may contribute substantially to the backscatter intensity (Wiebe and Greene, 1994; Holliday and Pieper, 1995; Stanton et al., 1993, 1994). However, analyses of patterns in biomass derived from ADCP backscatter intensity have demonstrated that the instrument provides reasonable and biologically meaningful descriptions of the biomass field and its association with hydrographic characteristics. Acoustic Doppler current profilers are particularly adept at documenting changes in the vertical distribution of biomass in the water column associated with the diel vertical migration of zooplankton and micronekton (Plueddemann and Pinkel, 1989; Buchholz et al., 1995; Heywood, 1996; Ashjian et al., 1998; Luo et al., 2000).

The diel vertical migration of acoustically derived biomass from the ADCP in the Arabian Sea is likely to be dominated by the migration of myctophid fish, since the region is characterized by these fish which produce a strong backscatter intensity signal, and, seasonally, by the vertically migrating pelagic crab *Charybdis smithii* (Currie et al., 1973; Nafpaktitis, 1978; Gjøsæter, 1981, 1984; Ropke et al., 1993; Van Couwelaar et al., 1997; Herring et al., 1998; Luo et al., 2000). The pelagic crab *C. smithii* has been observed in high abundance in the upper water column during both the SW and NE monsoons. This species ranges in length from 6–70 mm and should contribute substantially to the backscatter intensity when present. Comparison of backscatter intensity distributions collected simultaneously using a 153 kHz ADCP and 12 kHz sonar in the Arabian Sea suggested that the strongly migrating layers, observed by both acoustic instruments, were composed of fish whereas the non-migrating layers, seen only in the ADCP backscatter intensity, were attributed to zooplankton (Luo et al., 2000). Although mesozooplankton also migrate on a diel basis in this region (Smith et al., 1998b; Wishner et al., 1998), the larger size of the micronekton should produce most of the backscatter intensity signal for the vertically migrating

layers. Biomass in the upper water column should be dominated by non-migrating copepod species during day but overwhelmed by the biomass of vertically migrating fish and pelagic crabs at night. The vertically migrating myctophids and pelagic crabs are important predators because they feed primarily during night on zooplankton of the upper water column (e.g., Gjøsæter, 1984; Dalpadado and Gjøsæter, 1988; Kinzer and Schulz, 1991; Kinzer et al., 1993; Van Couwelaar et al., 1997).

The goals of the present study were to (1) document the seasonal changes in integrated biomass, particularly those associated with the changing monsoonal periods, across a 1000-km transect in the northern Arabian Sea, (2) contrast the magnitude and cycles of biomass inshore and offshore of the atmospheric Findlater Jet and also at a reference station located in the central Arabian Sea removed from the influence of the monsoons, (3) describe seasonal and spatial changes in the diel vertical migration behavior of the migrating biomass (myctophids, pelagic crabs), and (4) evaluate the potential predation pressure of these vertically migrating myctophids in the different regions. Because the acoustic Doppler

current profiler was operating continuously on the ten cruises of the Arabian Sea study, greater temporal (diel and seasonal) and spatial (horizontal and vertical) resolution and coverage of the distribution of plankton and nekton were achieved than was possible from the net-based sampling programs alone (Smith et al., 1998b; Wishner et al., 1998).

## 2. Methods

Ten cruises were conducted in 1994–1995 across a transect extending from near the coast of Oman (18°30'N, 57°18'E) to 1000 km offshore (14°27'N, 65°00'E) on the R/V *Thomas G. Thompson* during both the US JGOFS Arabian Sea Process Study and the Forced Upper Ocean Dynamics Program (Table 1; Fig. 1). Four of the cruises surveyed the transect line twice, resulting in 14 total transects. Data were collected continuously in 5 min averages using a hull-mounted, 153 kHz RD Instruments acoustic Doppler current profiler (ADCP). Most data were collected in 8 m depth bins, however 4 m depth bins were used over the shelf. The ADCP backscatter intensity data were calibrated and

Table 1  
Dates and cruise numbers of the 14 transects used in this study

Cruise–Transect	Dates	Season	Central Arabian Sea
TN042-outgoing	November 30–December 9, 1994	NE Monsoon	
TN042-ingoing	December 9–13, 1994	NE Monsoon	
TN043	January 17–31, 1995	NE Monsoon	*
TN044-outgoing	February 10–16, 1995	NE Monsoon	
TN044-incoming	February 16–21, 1995	NE Monsoon	
TN045	March 23–April 7, 1995	Intermonsoon	*
TN048-outgoing	June 26–July 4, 1995	SW Monsoon	
TN048-incoming	July 4–9, 1995	SW Monsoon	
TN049	July 30–August 11, 1995	SW Monsoon	*
TN050	August 30–September 12, 1995	SW Monsoon	*
TN051-outgoing	September 21–October 2, 1995	Intermonsoon	
TN051-incoming	October 2–5, 1995	Intermonsoon	
TN053	November 6–18, 1995	NE Monsoon	*
TN054	December 12–26, 1995	NE Monsoon	*

Cruises TN043, TN045, TN049, TN050, TN053, and TN054 were conducted as part of the US JGOFS study (National Science Foundation). Cruises TN042, TN044, TN048, and TN051 were conducted as part of the Forced Upper Ocean Dynamics Program (Office of Naval Research). The seasons of the monsoon sampled by each cruise are noted and, with the exception of TN044-incoming, are identical to those defined by Morrison et al., 1998. Cruises during which the central Arabian Sea station was sampled also are noted (\*).

range-corrected according to the methods of Flag and Smith (1989) and RD Instruments (1990). The ADCP data were entered into and accessed from a Common Oceanographic Data Access System (CODAS) database, developed by E. Firing at the University of Hawaii. The ADCP transducer on the *Thompson* is mounted on a pod that extends below the hull, producing a remarkably low-noise environment and one free of bubble interference from bubble-sweep-down. The range of the ADCP excluded the upper ~20 m of the water column because of the depth of the instrument on the hull of the ship and the blanking interval of the instrument. The deck unit of the ADCP was located in a climate-controlled laboratory that experienced constant temperature during the period of data collection.

During six of the cruises, a location far offshore in the Arabian Sea (10°00'N, 65°00'E), removed from the influence of the monsoons and the oxygen minimum zone, was sampled to serve as a reference point (station S15) (Fig. 1; Table 1). The ADCP data from this location were extracted and used to verify the consistency of the ADCP data over the course of the study period, and to establish a baseline of minimal seasonality in total biomass and diel vertical migration behavior to compare with those characteristics observed along the 1000-km transect line (Fig. 1). Examination of the backscatter intensity from this location revealed little variation in minimum intensity (noise), but a degradation in the penetration of the acoustic signal and depth range over the period of the study.

Vertically discrete zooplankton samples were collected using a 1 m<sup>2</sup> Multiple Opening/Closing Net and Environmental Sensing System (MOCNESS; Wiebe et al., 1976), equipped with 150 µm mesh nets, during three of the cruises (Smith et al., 1998b). These samples were used to derive an empirical relationship between backscatter intensity from the ADCP and zooplankton biomass. Zooplankton biomass was determined from the net plankton samples by first determining the displacement volume of each preserved sample using methods modified from Ahlstrom and Thrailkill (1963) and then converting the displacement volume to equivalent dry weight (mg/m<sup>3</sup>)

using the functional regressions of Wiebe et al. (1975) and Wiebe (1988). The biomass-intensity relationship was derived by comparing zooplankton dry weight from discrete depth ranges with spatially and temporally averaged coincident backscatter intensity data from the ADCP. The overall correlation between backscattered intensity, in dB, and log of the dry weight, in mg/m<sup>3</sup>, was 0.68. A Model 2 regression was used to convert all backscatter intensities (dB) in the database to approximate equivalent dry weight, using the following relationship:  $\text{Log}_{10}(\text{dry weight}) = 5.996 + 0.0662 \times \text{intensity}$ . Data from both day and night were utilized in deriving this relationship. It is likely that the 1 m<sup>2</sup> MOCNESS undersampled the night biomass because the net may not effectively capture fast swimming micronekton. Unfortunately, sampling with a net appropriate to capture fast swimming micronekton, such as a 10 m<sup>2</sup> MOCNESS, was not conducted from the *Thompson* during these cruises, so estimates of micronekton abundance were not available. Hence the biomass estimates derived from the regression, particularly for the data collected during the night, may underestimate the actual biomass present.

All data between the beginning and end points of the transect were extracted from the database without vertical or temporal averaging. The various cruise tracks frequently did not lie precisely along the transect. Excursions both along and off the transect occurred during stations and during the execution of grid surveys by towed instruments (cruises TN042, TN044, TN048, TN051) (Lee et al., 2000). Furthermore, station keeping resulted in multiple time periods being surveyed at a single location. Hence, a secondary data set consisting of data along the transect line was derived from the complete data set by removing observations collected during station keeping and then projecting the position of each off-track ADCP profile orthogonally back onto the transect line. The primary and secondary data sets were plotted as vertical sections as a function of time (primary data set) or distance offshore (secondary data set) for the 14 transects.

Integrated water-column biomass was calculated for both the 1000-km transect (edited data)

and the offshore station over a 20–120 m depth interval. Because the ADCP is not located at the sea surface, but mounted on the hull of the ship, data were collected only below 20 m. The depths to which reliable estimates of backscatter intensity (% good > 92; e.g., Flagg and Smith, 1989) were obtained shoaled dramatically during night, presumably because of the absence of scatterers in deeper layers due to upward diel vertical migration (Flagg and Kim, 1998; similar pattern observed by Herring et al., 1998). Hence, only those profiles that extended to 120 m were considered in this analysis to ensure that backscatter intensity measurements were present for all depths considered when integrating and comparing biomass. Because of the strong diel signal, day and night integrated biomasses were considered separately.

Day and night integrated biomasses and chlorophyll *a* concentrations were further processed by objective analysis (OA) according to the method of Mariano and Brown (1992) to calculate predation pressure indices and to regress daytime biomass on chlorophyll *a* concentration. Objective analysis is useful in projecting data collected asynchronously onto temporally and spatially uniform fields. A modified format was adopted to analyze the averaged data over distance (1000-km along transect) and time (180 days) for all cruises. The observation variable (i.e. daytime biomass, nighttime biomass, chlorophyll *a* concentration) was decomposed into a mean field, a natural variability (mesoscale) field, and a subgrid-scale noise error field (for equations, see Mariano and Brown, 1992). The mean field was estimated by a two-dimensional bicubic spline with adjustable smoothness and tension parameters. The mean distributions were removed from the data before OA calculations. An interpolation grid was defined based on the number of points and resolution in space and time for the output field estimate (101 × 101 grid, 0.01° resolution). At each grid point, a weighted local average of the influential detrended data points was calculated and subtracted from each influential detrended data point. The output for each variable was an OA field of identical spatial and temporal extent calculated from the sum of the OA estimate, the local average, and the trend, and a trend field (deviation

from the data field) based on field variance, sensor error, and the uncertainty in the estimation of the mean.

Diel vertical migration (DVM) in the data was identified by examining the vertical distribution of biomass relative to the timing of day and night over the sampled water column. The median depth (depth at which 50% of the biomass is located above and below) was selected to represent the vertical distribution of biomass in the water column and to identify periods of diel vertical migration (e.g., Ashjian et al., 1998). This statistic best represented the observed vertical distribution of biomass of the several statistics considered (depth of maximum biomass, mean depth). Use of a single statistic to represent vertical distribution could be misleading if multiple migrating scattering layers were observed, such as seen in Luo et al. (2000). For the present data, only single migrating layers were observed. The median depth was calculated for all data collected during a transect (no removal of data points because of station keeping or excursions from the transect line). Potential along-track variation in migration behavior was examined by comparing vertical distributions from different along-track locations for each cruise.

Vertical migration velocities were calculated from the median depth of biomass. The median depth first was smoothed over time using a 10-point running mean (~50 min) to reduce small-scale variation. Vertical migration velocities then were calculated between each successive data point as the change in depth (m) per time period (s). Most observations were separated by 5 min intervals except when a profile was missing from the data because of poor quality.

Periods when diel vertical migration (DVM) was strong were identified using a DVM Index. This index reflects the adherence of the vertical distribution of the median depth to a sinusoid curve (e.g., Pearre, 1979), which approximates the diel changes in depth of isolumens through the water column. Before calculating the index, the vertical distribution of the median depth for each day was time-standardized so that sunrise and sunset occurred at 0600 and 1800, respectively, and depth-normalized to a range of 0–1 so that the maximum median depth was set to 1 and the

minimum to 0 (e.g., Ashjian et al., 1998). An “ideal” distribution then was calculated for each day by converting the observed times of each profile to equivalent radians and calculating the cosine function of the sinusoid curve. The sum of squares (SS) of the deviation then was calculated for each day and used as the DVM index:

$$\text{dev.SS} = \frac{1}{N-1} \sum_i^N (\text{observed median depth}_i - \text{predicted median depth}_i)^2,$$

for  $i = 1$  to  $N$ , where  $N$  is the number of profiles in that day. Therefore, a lower value of the DVM index indicates greater adherence to an ideal DVM distribution, as simulated by a sinusoid.

The vertical range of the acoustic data was limited during both day and night for the last two cruises (November 1995 (TN053); December 1995 (TN054)). Because of an apparent degradation of the ADCP signal, the DVM index was not calculated for December 1995 (TN054). Examination of the vertical sections of intensity from the reference station located in the central Arabian Sea over the period of the study demonstrated that, although the depth range of the instrument clearly was reduced, the magnitude of the intensity did not appear to be affected. Comparisons involving the magnitude of biomass from November and December 1995 were considered with care.

Statistical analyses were conducted using MATLAB (Mathworks, Inc.) or the Statistical Analysis System (SAS; SAS Institute, Inc., 1985). For multiple comparisons of means, analysis of variance was used to identify whether significant differences existed and the Student-Newman-Keuls post-hoc test was used to identify which means or groups of means were significantly different (Zar, 1984).

### 3. Results

#### 3.1. Vertical distribution of acoustically-derived biomass

The vertical distributions of acoustically-derived biomass (hereinafter ADCP biomass) as a function

both of along-transect distance (Fig. 2a) and of time (Fig. 2b) from the March–April, 1995 cruise are shown as examples of typical vertical sections observed for the 14 transects. A strong diel vertical migration signal was the prevalent feature of the vertical distribution for all of the cruises, with only a single migrating layer observed. Greatest biomass was observed near the surface during night and at depth (>250 m) during day. Strong and rapid vertical redistributions of biomass as a single coherent mass were associated with periods of sunrise and sunset. Most profiles collected during day extended quite far into the water column. The penetration of the acoustic signal to depth was limited during night because of the aforementioned absence of sound scatterers (zooplankton and micronekton). The along-transect vertical distribution (Fig. 2a) demonstrates the temporal discontinuities resulting from station-keeping and the editing of the data.

The vertical distribution of the median depth clearly showed the effect of DVM on the distribution of biomass, following a sinusoid pattern throughout the 24 h, and was an effective means of representing the vertical distribution of the biomass (Fig. 2b, upper panel). Occasionally, the median depth of biomass deviated from this pattern when the biomass signal was reduced (e.g., Fig. 2b, day 28). Vertical velocities (Fig. 2b, lower panel) showed prominent peaks of upward or downward movement (migration) associated with times of sunset or sunrise, respectively.

#### 3.2. Spatial and temporal distribution of ADCP biomass

The ADCP biomass present in the upper 120 m during day was considered to be zooplankton, while that present during night was considered to be zooplankton plus those organisms that migrate to the upper 120 m during night, primarily myctophid fish, swimming crabs, and euphausiids. Because of the different compositions of the biomass, day and night distributions and patterns of biomass were considered separately. The influence of the SWM (June–September, 1995) was clear in the along-transect distribution of vertically integrated (20–120 m) zooplankton

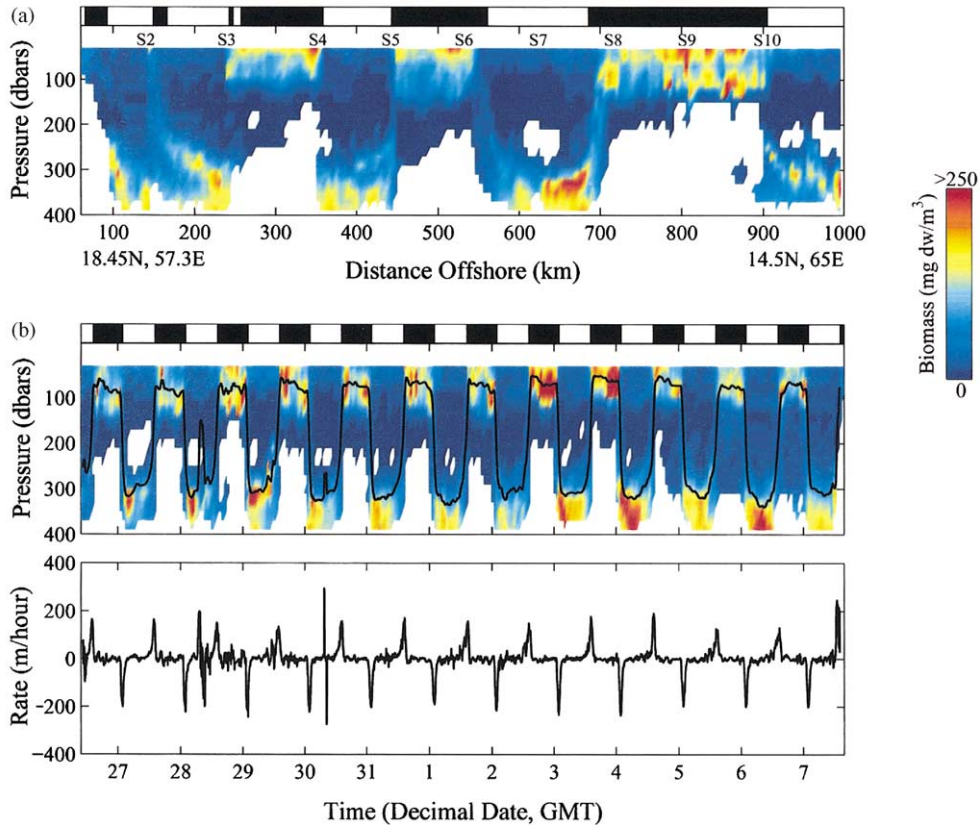


Fig. 2. Vertical distributions of biomass from March–April, 1995 (TN045) as a function of along-track distance ( $n=585$  profiles) (upper panel), and time ( $n=3447$  profiles) (middle panel). Periods of day (white) and night (dark) are shown in the bars across the top of each panel. The median depth of biomass as a function of time also is shown (black line). The lower panel shows the rate of vertical displacement of the median depth of biomass, calculated after applying a 10-point running mean. Vertical profiles were gridded to a density of 1 point/20 m in the vertical and 1 point/5 km for distance or 1 point/h for time in the horizontal. The along-track locations of standard US JGOFS process study stations (S2–S10) are shown as reference (upper panel).

biomass throughout the year (Fig. 3a). Elevated zooplankton biomass was observed inshore (stations S2–S5) of the Findlater Jet (Jet located between stations S6 and S7; see Fig. 1) during late June–early October, extending offshore to the Findlater Jet region during a single cruise in August. Peak zooplankton biomass was observed in July at station S3, with the greatest areal extent of enhanced biomass occurring during the late SWM (September). Elevated night ADCP biomass (the sum of zooplankton and migrator biomasses) was observed offshore during the NEM and Spring Intermonsoon (SI) periods from December to April (Fig. 3b). Elevated night ADCP biomass

also was observed inshore of the Findlater Jet during the SWM (July); this peak corresponds with the peak in zooplankton biomass.

When the mean, vertically integrated ADCP biomass for regions inshore (stations S2–S4; 104–403 km along-transect) and offshore (stations S7–S11; 584–1064 km along-transect) of the Findlater Jet for each sampling period are compared, seasonal patterns emerge (Fig. 4). Biomass was significantly greater during night (migrators plus upper-ocean zooplankton) than day (upper-ocean zooplankton only) for each sampling period within each region (ANOVA,  $p < 0.0001$ ). Similar temporal patterns were

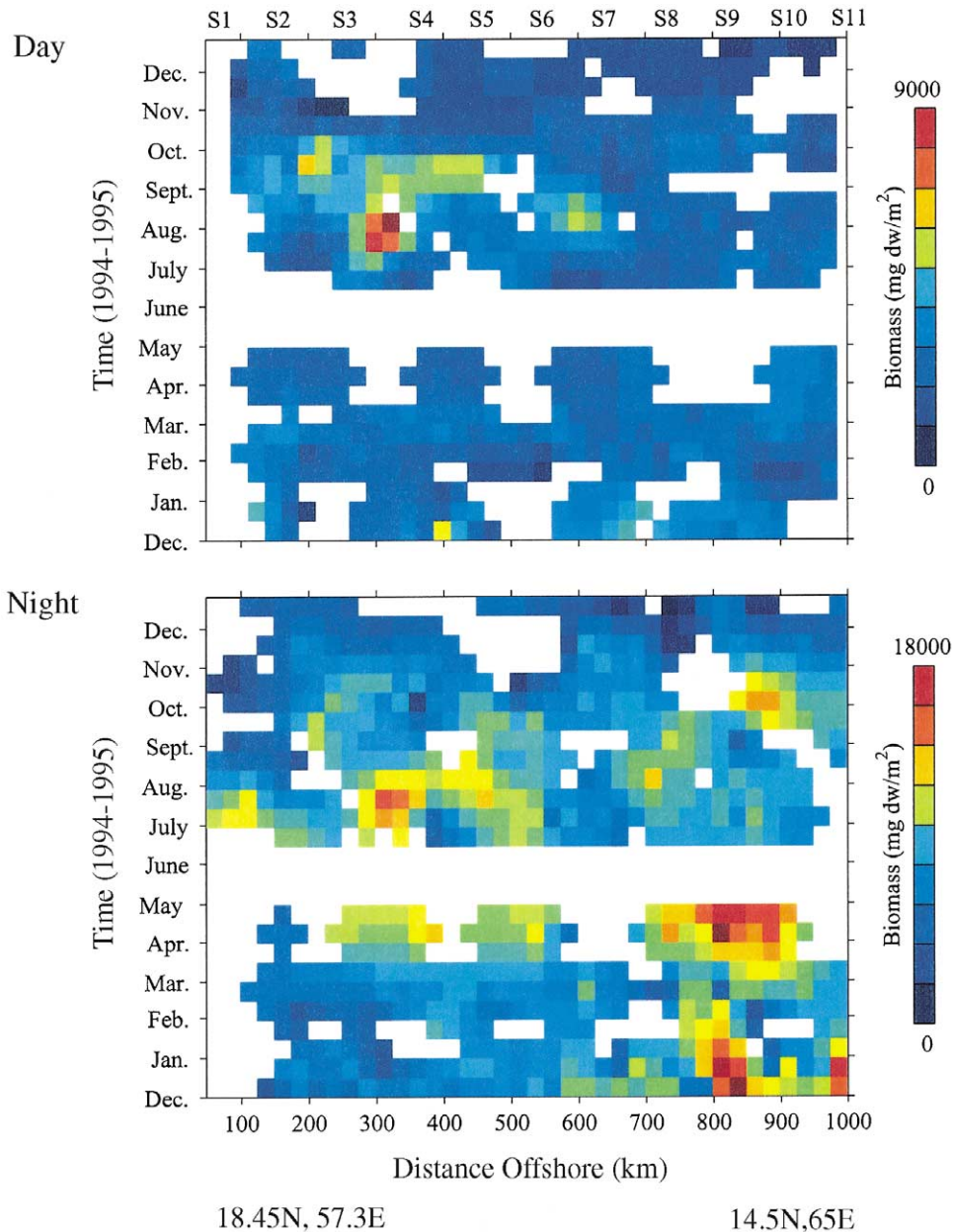


Fig. 3. Annual distribution of integrated ADCP biomass in the upper water column (20–120 m) for day (upper) and night (lower) as a function of along track distance and time. The along-track locations of the standard US JGOFS process study stations (S1–S11) are shown as reference. Data were gridded to a density of 1 point/15 days in the vertical and 1 point/25 km in the horizontal. Gaps in the distribution resulted when along-transect locations were not sampled during that period (day or night). Note the scale change between day and night. No cruises took place in May and most of June 1995.

observed for both zooplankton and zooplankton plus migrators within each region. Greatest biomass inshore was observed during the SWM,

intermediate biomass during the 1994 NEM, and lower biomass during the fall 1995 NEM (ANOVA,  $p < 0.001$ ; Student Newman Keuls (SNK),

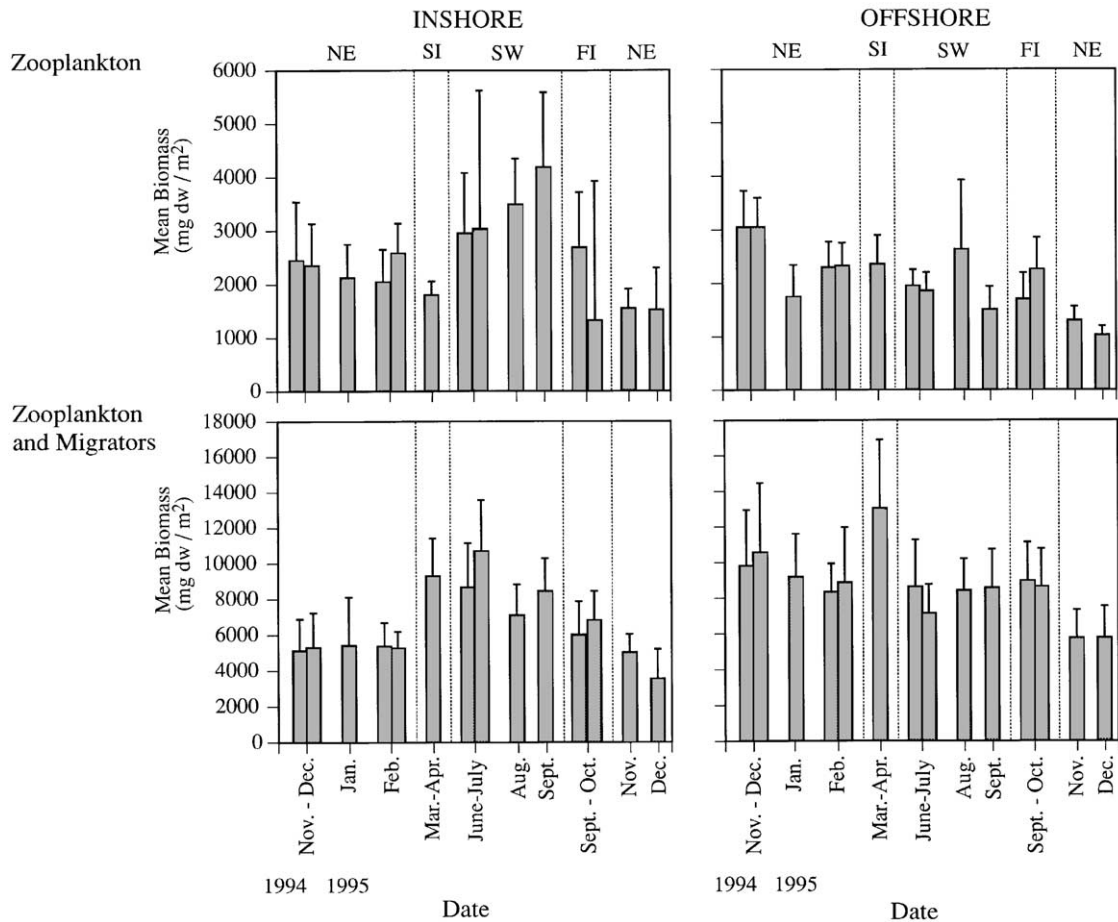


Fig. 4. Average biomass in the upper water column (20–120 m) for regions inshore (S2–S4; 104–403 km from shore) and offshore (S7–S11; 584–1064 km from shore) of the atmospheric Findlater Jet along the transect line during day (zooplankton) and night (zooplankton and migrators). Only those profiles extending down to 120 m were used. Standard deviations are shown with the error bars. Each mean was calculated utilizing 392–659 profiles. Separate means are calculated for each leg for cruises with both an incoming and outgoing leg. The periods of the Northeast Monsoon (NE), Spring Intermonsoon (SI), Southwest Monsoon (SW), and Fall Intermonsoon (FI) are separated by dashed lines.

$p < 0.05$ ). The patterns of both types of biomass offshore were the reverse, with greatest biomass generally observed during the fall 1994 NEM and Intermonsoon periods, lower biomass during the SWM, and lowest biomass during the early NEM in 1995 (ANOVA,  $p < 0.001$ ; SNK,  $p < 0.05$ ). For repeat transects within a cruise, biomasses usually were similar, suggesting that spatial and temporal patchiness had little effect for those periods. Biomasses were lowest during November and

December 1995 for all four region/diel period groupings (with the exception of September–October 1995, but see large variability in mean). This may have resulted from interannual variability in biomass between the two years or may be a consequence of the degradation of the ADCP signal at the end of 1995 (see methods section).

Averages of integrated biomass (20–120 m) at the central Arabian Sea offshore station (S15) were compared to averages from the regions inshore

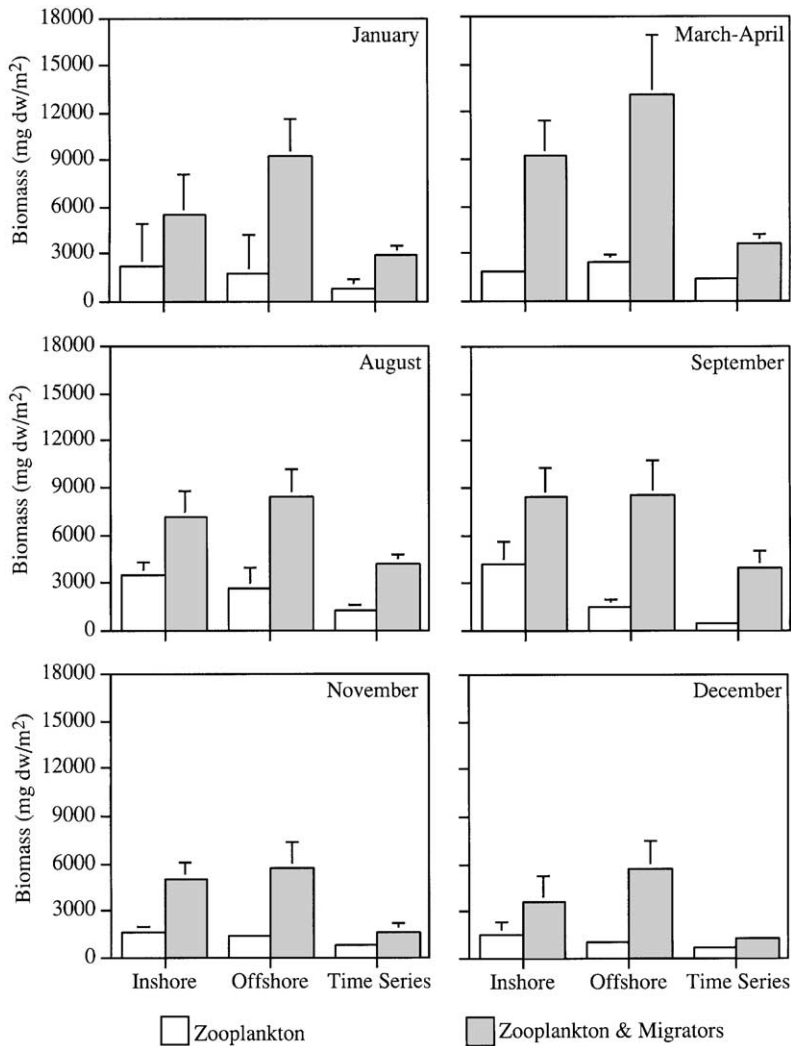


Fig. 5. Average integrated biomass (20–120 m) during day and night for the regions inshore and offshore of the Findlater Jet and the time-series station. Error bars show standard deviations. Because common ranges were used for the y-axis for all plots, small standard deviations do not show; for inshore and offshore these can be seen in Fig. 4. Only those profiles extending to 120 m were used in calculation of the means. For most cases, greater than 100 profiles were included in each calculation (range: 34–286). Because of degradation of the vertical range of the instrument during the last two cruises (November and December), fewer profiles (9–170) were available for inclusion in the calculation for these periods.

and offshore of the Findlater Jet for the months during which all three locations were sampled (Fig. 5). The spatial pattern of upper-ocean zooplankton biomass suggested a general, persistent, decreasing gradient from inshore regions (stations S2–S5) to the central Arabian Sea (station S15). Greatest zooplankton biomass

(day) was seen in the inshore region (stations S2–S5), with intermediate levels in the offshore region (stations S7–S11), and lowest biomass at the central Arabian Sea station (S15) for five of the months during which all three regions were sampled (Fig. 5); the single exception to this pattern was March–April when biomass in the

offshore region exceeded that seen in the inshore region (ANOVA,  $p < 0.0001$ ; SNK,  $p < 0.05$ ). In contrast, greatest night biomass was observed in the region offshore of the Findlater Jet, with intermediate biomass inshore of this feature, and lowest night biomass in the central Arabian Sea (station S15) (ANOVA,  $p < 0.0001$ ; Fig. 5). Night biomass was significantly different within each of the three regions for each time period with the exception of September, when similar biomass levels were observed in the inshore and offshore regions (ANOVA,  $p < 0.0001$ ; SNK,  $p < 0.05$ ; Fig. 5).

### 3.3. Temporal variability in biomass: the time-series station in the central Arabian Sea

Despite an initial assumption of limited seasonality in the central Arabian Sea, significant temporal differences were observed at the time-series station (S15) among different sampling months for both zooplankton and night biomasses (ANOVA;  $p < 0.0001$ ) (Fig. 5). For zooplankton, greatest biomass was observed during March–April (SI) and August (SWM), lowest biomass in September (SWM), and intermediate biomass during January (NEM) and November (NEM) (Student-Newman-Keuls post-hoc test). In contrast, greatest night biomass was observed during August (SWM) and September (SWM) (means not significantly different), with intermediate biomass during January (NEM) and March–April (SI), and lowest biomass during November (NEM) and December (NEM) (all means significantly different). Hence, significant variability throughout the year was observed at station S15 where seasonal variability had previously thought to be negligible. Night biomass was significantly greater than zooplankton biomass alone for all periods (ANOVA;  $p < 0.0001$ ).

### 3.4. Abundance of predators versus non-migrating zooplankton

Migrator biomass was calculated as the difference between day ADCP biomass and night ADCP biomass present in the upper 120 m. The taxa believed to have produced the night ADCP

biomass (myctophids, pelagic crabs, euphausiids) all utilize mesozooplankton as prey. Migrator biomass was greater offshore than inshore of the Findlater Jet for all periods (Wilcoxon's Signed Rank Test;  $p < 0.005$ ), with the exception of July when migrator biomass in the two regions was similar (Fig. 6). In the inshore region (stations S2–S5), lowest migrator biomass was observed during the NEM and elevated migratory biomass occurred during the Spring Intermonsoon and the SWM. Migrator biomass was lowest at station S15 in the central Arabian Sea. A decline in migrator biomass was observed in the last two cruises (Fig. 6; November and December 1995). Although this may have been a consequence of the reduced capabilities of the ADCP instrument during these cruises, migrator biomass of the inshore area in December 1994 equaled that of December 1995.

The ratio of inshore to offshore biomass for each period demonstrated the relative magnitudes of zooplankton biomass and migrator biomass in the two regions (Fig. 7). Significant differences between inshore and offshore regions were observed for all except two comparisons for both day and night ADCP biomass (ANOVA,  $p < 0.024$  or better). Zooplankton biomass was not greatly different in the two regions during the NEM and SI seasons (ratio was  $\sim 1 \pm 0.2$ ). However, zooplankton biomass inshore greatly exceeded biomass offshore during the SWM (by a factor of 1.5 during August). The ratio dropped off sharply at the end of the SWM but was greater than one during the early NEM (November and December). Both night and migrator biomasses were lower in the inshore region relative to the offshore region, with the exception of a single transect early in the SWM (June–July).

### 3.5. Predation pressure

The potential predation impact of the vertically migrating myctophid fish and pelagic crabs on the zooplankton community of the upper 120 m was assessed using a predation pressure index for the regions inshore and offshore of the Findlater Jet and for the central Arabian Sea station. For the data collected along the transect, as well as the offshore station, the calculation of this index used

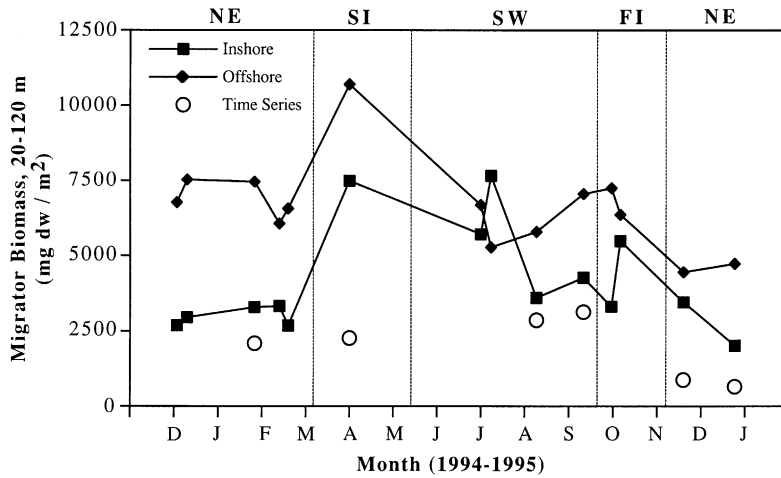


Fig. 6. Migrator biomass in the upper water column (20–120 m) for regions inshore (S2–S4; 104–403 km from shore) and offshore (S7–S11; 584–1064 km from shore) of the Findlater Jet along the transect line and at the time-series station in the central Arabian Sea along the transect line. Migrator biomass was calculated using the mean integrated day and night ADCP biomass for each region for each cruise and subtracting day biomass from night biomass; this removed the biomass portion in the night data that consisted of non-migrating upper water-column zooplankton. Monsoonal cycle indicated as in Fig. 4.

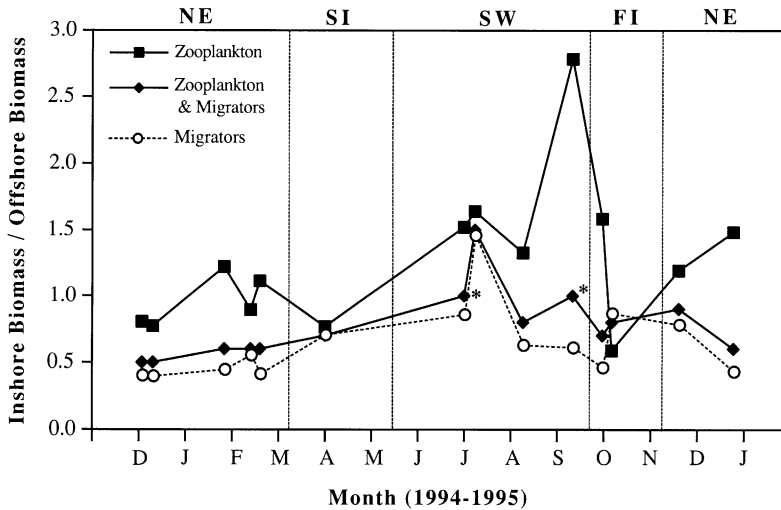


Fig. 7. Ratio of inshore to offshore day, night, and migrator biomass for each of the 14 transects. Ratios were calculated using the mean integrated ADCP biomass (20–120 m) for the inshore (S2–S4; 104–403 km from shore) and offshore (S7–S11; 584–1064 km from shore) regions for each cruise for day and night separately. Times for which there was no significant difference between inshore and offshore biomass are indicated by an asterisk; all other inshore versus offshore comparisons were significant (ANOVA,  $p < 0.024$ ). Monsoonal cycle indicated as in Fig. 4.

the mean day and night biomass values from objective analysis matrices for each region observed during each transect of the study and

reflected the relative magnitude of the day versus night biomass levels. The reason for using objectively analyzed data matrices was to

interpolate data from day and night ADCP biomass estimates to obtain overlapping values for specific positions along the transect.

The predation index was calculated as:

$$\text{PPI} = (B_n - B_d) / B_d$$

where  $B_n$  = night biomass and  $B_d$  = day biomass.

The indices for all transects considered in a comparison were normalized to the maximum index found, so that the range of indices within a comparison ranged from 0 to 1.

The predation pressure index (PPI) was greater offshore (0.5–1.0) than inshore (0.2–0.6) of the Findlater Jet ( $p < 0.05$ , Wilcoxon's Paired Sample Test; Zar, 1984) (Fig. 8). The PPI was greatest during the SI period (March) for both inshore and offshore regions. Predation pressure also was elevated during the late SWM and Fall Intermonsoon periods, especially for the region offshore of the Findlater Jet.

Predation pressure at the offshore station, with the exception of a single observation (September), was similar to that observed inshore of the Findlater Jet (Fig. 8) and lower than that observed offshore of the Jet, at least for the six months for which all three locations were sampled (Kruskal–Wallis test;  $p < 0.01$ ; Student–Newman–Keuls type nonparametric multiple comparison of means,  $p < 0.05$ ). With the exception of September, the predation pressure index at the time-series station (S15) was fairly constant.

### 3.6. Zooplankton biomass and chlorophyll *a* fluorescence

Upper-ocean zooplankton biomass was compared to chlorophyll *a* fluorescence for stations inshore of the Findlater Jet during the SWM (Gunderson et al., 1998) (Fig. 9). Because of sparse sampling, objective analysis was used as a means to interpolate the irregularly spaced raw data onto a regular grid; fluorescence and zooplankton biomass data at coincident interpolated locations then were compared. A strong negative correlation, with small variance, was observed between chlorophyll *a* fluorescence and upper-ocean zooplankton biomass. Chlorophyll *a* fluorescence was

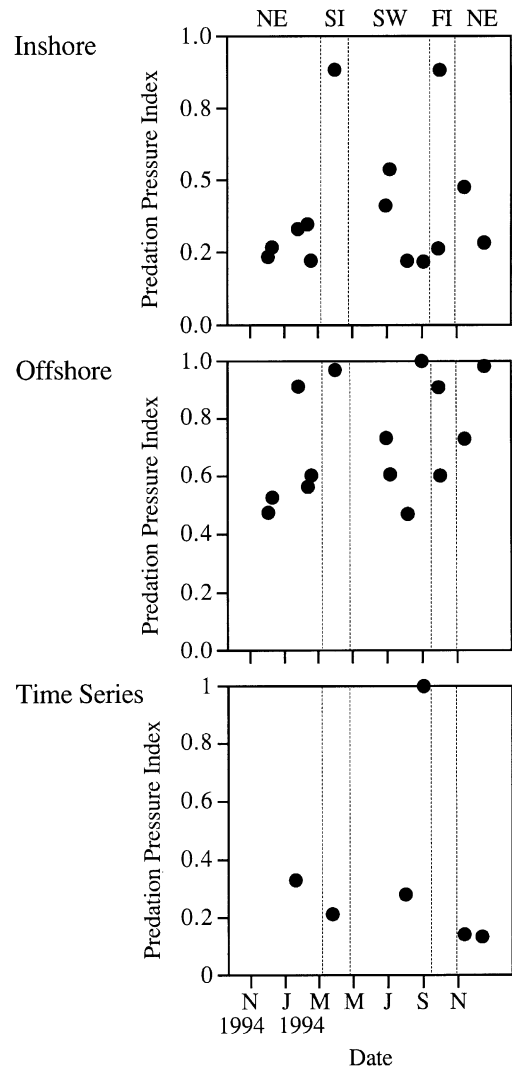


Fig. 8. Predation pressure index for the regions inshore and offshore of the Findlater Jet during each transect of the study and at central Arabian Sea time-series station for six periods when this site was surveyed. Raw indices are normalized to the maximum index observed so that index ranges from 0–1.0. Monsoonal cycle indicated as in Fig. 4.

low in the region where low temperature and elevated nitrate indicated upwelling, a pattern also found in the upwelling area off Somalia (Smith and Codispoti, 1980) and Peru (Boyd and Smith, 1983). However, unlike Peru where high chlorophyll *a* and zooplankton abundance co-occur on the offshore and downstream edges of the

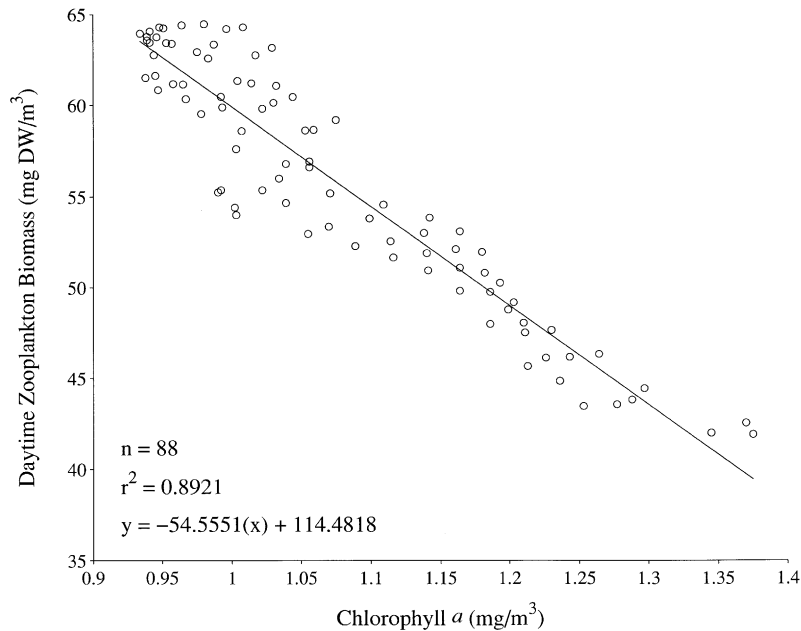


Fig. 9. Comparison of chlorophyll *a* fluorescence and upper-ocean zooplankton biomass from a region inshore of the Findlater Jet during the SWM.

upwelling area (Boyd and Smith, 1983), in this study the area of the highest concentration of zooplankton coincided spatially with the area of low chlorophyll *a* fluorescence. A similar distribution of zooplankton biomass, high in the area of low chlorophyll *a*, also was observed off Somalia (Smith, 1982; Baars and Oösterhuis, 1997). Grazing by zooplankton may have been responsible for the low concentrations of chlorophyll *a* fluorescence observed in this region, as has been suggested for Somalia (Baars and Oösterhuis, 1997). The season and area in which these grazing effects were seen off Oman are the times and places where the microbial loop is the most unbalanced (Landry et al., 1998) and where large-sized phytoplankton predominate (Garrison et al., 2000; Smith, 2001).

### 3.7. Diel vertical migration: an index of DVM

The diel vertical migration (DVM) index reflected the presence and strength of diel vertical migration of myctophids, swimming crabs, and euphausiids across the transects. The predicted

vertical distribution of the normalized median depth of biomass during DVM was represented by a sinusoidal curve that closely tracked the observed vertical distribution during periods when DVM was occurring (e.g., March–April; upper panel, Fig. 10) but was clearly different during periods when DVM was weak or absent (e.g., June–July; lower panel, Fig. 10). Periods with a strong DVM pattern then were characterized by low diel vertical migration indices, since this was calculated as the sum of squares, and days with weak diel signals were characterized by higher DVM indices.

Variation in the strength of diel vertical migration was observed between different sampling periods (Fig. 11; ANOVA  $p < 0.0001$ ) but not between different regions across the transect within a sampling period. The DVM index was significantly greater during the June–July period early in the SWM than other periods (SNK;  $p < 0.05$ ), indicating that the vertical distribution of biomass did not exhibit as strong a diel vertical migration pattern during the SWM as it did during other months. Strongest diel vertical migration

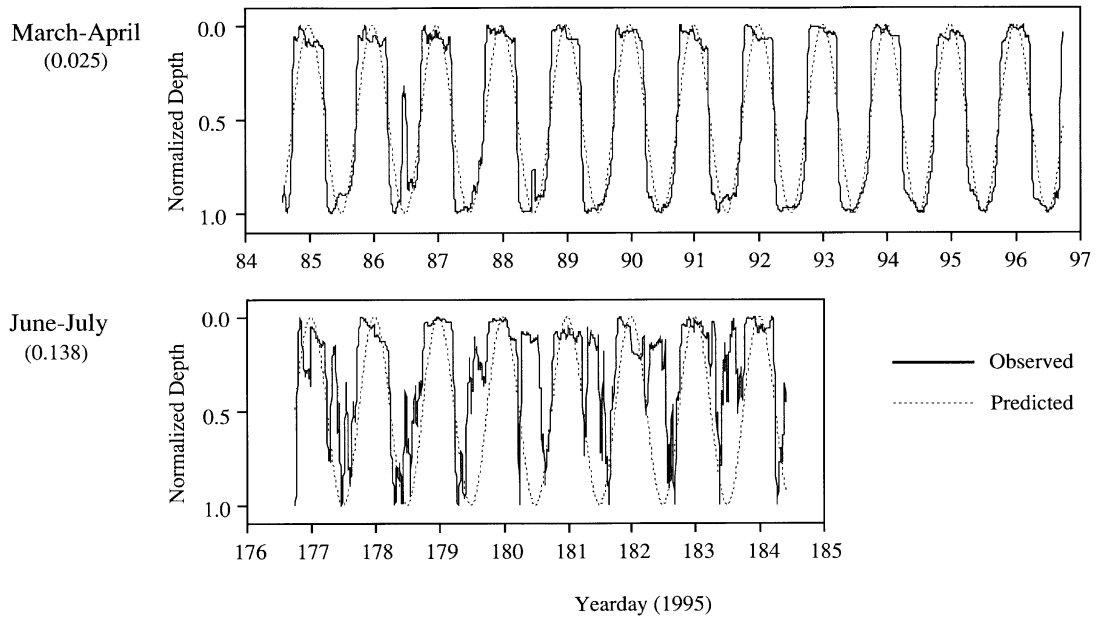


Fig. 10. Examples of the observed and predicted (sinusoid) vertical distributions of the normalized median depth used in calculation of the diel vertical migration (DVM) index during periods of strong (upper panel) and weak (lower panel) DVM. The mean DVM index for each period is also shown in parentheses.

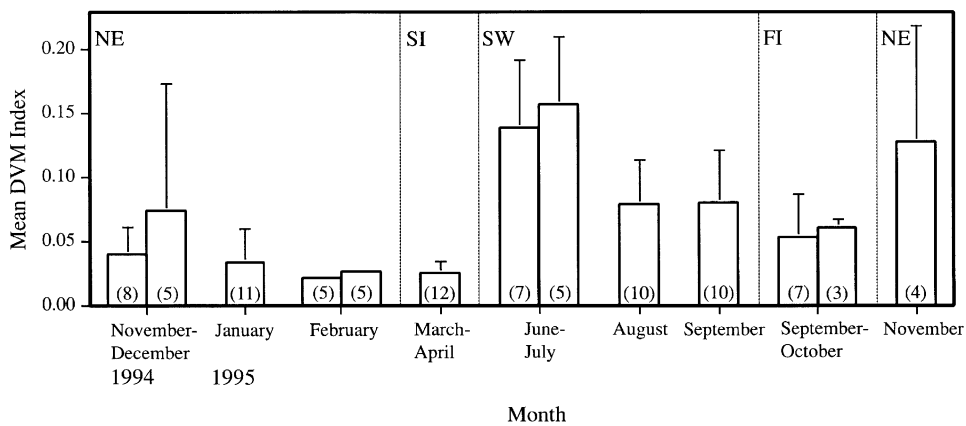


Fig. 11. Average diel vertical migration index for each transect. Lower values of the index indicate greater adherence of the observed vertical distribution of biomass to that expected for diel vertical migration. Error bars indicate one standard deviation and numbers within each column indicate the number of observations (*n*) used to calculate the mean. The different seasons of the monsoon cycle indicated as in Fig. 4.

was seen during the NEM and SI in early 1995. Visual examination of vertical sections of biomass from these periods confirmed the classification of the index. For the time-series station in the central

Arabian Sea, the DVM index was lower than 0.10 (indicating strong DVM) for six out of the ten days that were sampled during January, March–April, August, and September (not shown). Some

days in November and December also exhibited low indices, indicative of DVM; however, fewer observations were available during these months because of the degradation of the ADCPs range. It is likely that DVM was present during these months as well.

3.8. Diel vertical migration: migration velocity

Vertical migration velocities, calculated using only days when a diel vertical migration index of <0.1 was observed, varied significantly

throughout the year (Fig. 12; ANOVA,  $p < 0.001$ ). Migration velocities were not calculated for the transect in July 1995 (TN048-incoming, poor adherence to a diel vertical migration pattern for all days) or for the last transect in December (TN054, degradation of ADCP signal). Greatest velocities (~300–500 m/h) were observed during the NEM of early 1995 and the Fall Intermonsoon of 1995 (SNK,  $p < 0.05$ ). No consistent regional (inshore/offshore) patterns during a cruise were observed. Furthermore, when all cruises were considered together, no consistent differences

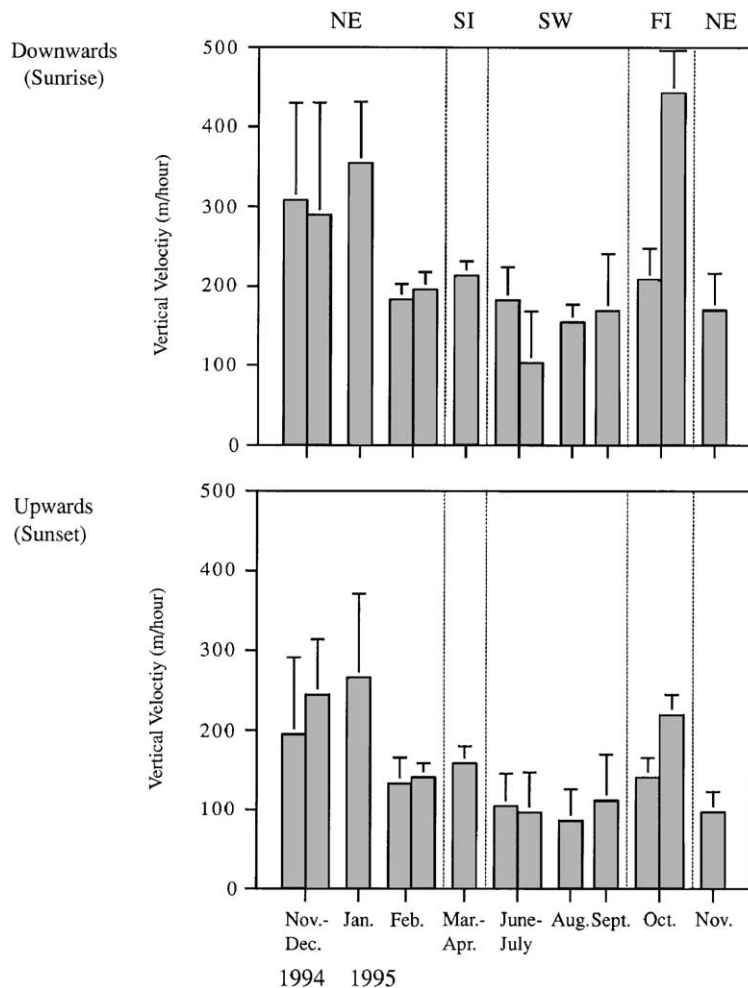


Fig. 12. Average peak vertical velocities during downward (sunrise) and upward (sunset) migrations for each cruise. Error bars indicate one standard deviation. The different seasons of the monsoon cycle indicated as in Fig. 4.

among regions were found (ANOVA,  $p > 0.5$ ). Downward migration velocity exceeded upward migration velocity for 7 of the 12 periods considered (ANOVA,  $p < 0.05$ ).

### 3.9. Diel vertical migration: timing of migration

On average, the timing of both upward and downward peak migrations preceded the astronomical sunset and sunrise times, respectively (Fig. 13). No significant differences were seen in the timing of migration relative to sunrise and sunset between downward and upward migrations, respectively (ANOVA). For the downward migration at sunrise, differences between the different cruises and also between regions were observed.

Peak downward migration was more closely associated with the time of sunrise offshore of the Findlater Jet than inshore of the Jet (ANOVA,  $p < 0.001$  and  $0.002$ , respectively). Generally, downward migration preceded sunrise during the NEM and occurred after sunrise during the SWM and Intermonsoon periods. The pattern was not completely consistent, and it is unclear from the data available whether these differences resulted from changes in the migrating community composition or meteorological conditions (e.g., clouds) that could have altered the light levels perceived by the organisms. For the upward migration at sunset, no differences in timing were observed between regions or cruises throughout the 16 months of observation.

## 4. Discussion

### 4.1. Zooplankton biomass

The effect of the SWM on zooplankton biomass was confined to the region inshore of the Findlater Jet (Fig. 3). Such an elevation has been observed both in previous studies in the region (e.g., Smith, 1982; Van Couwelaar et al., 1997) and also in data collected using nets during this study (Smith et al., 1998b; Wishner et al., 1998). Overall, zooplankton biomass inshore of the Findlater Jet during the SWM was 1.6 times greater than that observed during the NEM of 1994–1995 and 2.3 times greater than that observed during the NEM of 1995–1996. Zooplankton biomass during NEM periods inshore of 600–700 km was similar in magnitude to the Intermonsoon periods. Much of the increased biomass that occurred in the upwelling region during the SWM likely was composed of the ontogenetically migrating copepod species *Calanoides carinatus*, which migrates upward during this period to reproduce (Smith et al., 1998b). Other large-bodied copepod species that contributed to the nearshore upwelling zooplankton community include *Calanus minor*, *Eucalanus crassus*, *E. elongatus*, and *Heterostylites longicornis*, as well as the numerically dominant but smaller *Pleuromamma indica* (Smith et al., 1998b). The potential grazing impact of the

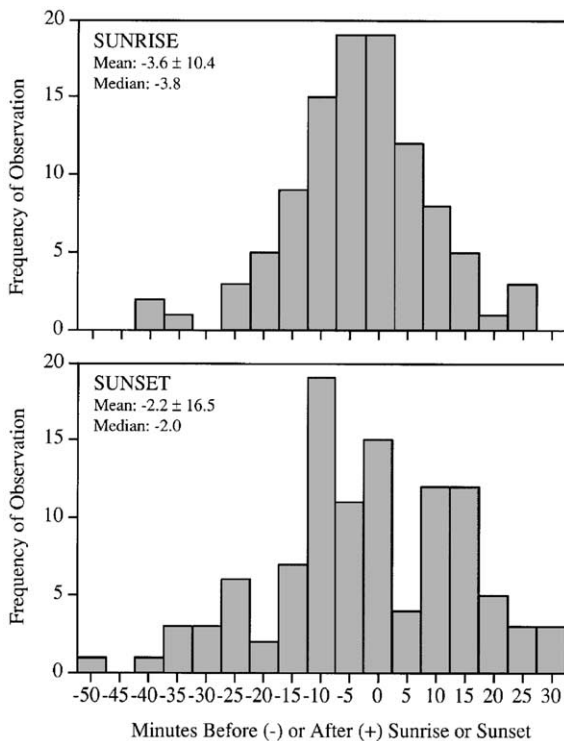


Fig. 13. Timing of peak upward and downward migration velocities relative to the times of astronomical sunset and sunrise, respectively. The difference in minutes between the time of the peak velocity and the astronomical time of sunrise/sunset was calculated; negative values indicate that migration preceded sunrise/sunset.

zooplankton community on phytoplankton, as demonstrated by the inverse relationship between chlorophyll *a* concentrations and zooplankton biomass, with low chlorophyll *a* concentrations during periods of elevated nutrients (SWM), suggests also that this ontogenetic migration coincided with elevated food levels for the copepods. The zooplankton community in this region may have evolved life histories that are exquisitely timed to exploit the predictable appearance and conditions of the SWM.

In contrast, the offshore region exhibited much reduced variation in biomass, with greatest values observed during the NEM. Except during the SWM, the magnitude of zooplankton biomass was not greatly different in the inshore and offshore regions (Figs. 4 and 6), suggesting that zooplankton biomass remained fairly constant for much of the year. This apparent lack of seasonality, termed the “Arabian Sea Paradox”, has been observed both in previous studies and by investigators utilizing net-sampling during the 1994–1995 expedition (e.g., Madhupratap et al., 1996a,b; Wishner et al., 1998). Surprisingly, the zooplankton biomass at the central Arabian Sea station changed during the year, although the magnitude of the variation was less than elsewhere and zooplankton biomass at that site was considerably and consistently lower than either the inshore or offshore regions.

A strong onshore–offshore decreasing gradient in zooplankton was a persistent feature in net-based studies, including those that occurred coincident with the present study (Qasim, 1977; Smith et al., 1998b; Wishner et al., 1998). An onshore–offshore decline in zooplankton biomass was observed in the ADCP data for three of the four months considered in the Smith et al. (1998b) and Wishner et al. (1998) studies, with the greatest contrasts existing during the SWM (inshore region 2.8 times that offshore of the Findlater Jet and 9.6 times that at the central Arabian Sea station). However, this gradient was not observed consistently in all regional comparisons of zooplankton biomass estimated using the ADCP (Figs. 5 and 6). The greater temporal resolution of the ADCP-based survey relative to the net-based studies revealed that the onshore–offshore gradient

was not consistent and that zooplankton biomass did not vary greatly among different regions during all periods of the year. The present study’s strengths are its ability to resolve the spatial extent of the region of elevated biomass and to evaluate the magnitude of the response with sufficient observations to perform meaningful statistical tests.

Zooplankton biovolume and biovolume estimated using high-frequency acoustics during the SWM, NEM, and FI of 1995 showed different seasonal and across-transect trends (Pieper et al., 2001) than those observed both from net studies (Smith et al., 1998b; Wishner et al., 1998) and the ADCP (this study). Differences between results of the acoustic (Pieper et al. 2001) and net (Smith et al., 1998b; Wishner et al., 1998) studies were attributed to the more effective sampling of the smallest size class (0–0.16 mm ESR or 0.2–0.8 mm length) by the high-frequency acoustics relative to the MOCNESS, which sampled a larger size class (0.34–0.7 mm ESR or 2.0–4.2 mm length) most effectively (Pieper et al., 2001). The ADCP likewise may have sampled larger size classes more effectively than the high-frequency acoustics since seasonal and spatial patterns similar to those of the net-based biomass studies were observed with the ADCP and zooplankton of those size classes theoretically should be effective sound scatterers at the frequency of the ADCP instrument.

#### 4.2. Migrator biomass

Migrator biomass varied throughout the year along the 1000-km transect, but the pattern of variation over the year was similar both inshore and offshore of the position of the Findlater Jet in the SWM (600 km from the coast of Oman). Greatest migrator biomass was observed during the SI and SWM, with reduced levels during the FI and NEM. The enhancement of migrator biomass may have resulted either from in situ production, such as during an annual reproduction cycle, from behavioral changes that resulted in greater numbers of individuals migrating during the SI and SWM, or from changes in the size frequency distribution of the sound-scattering migrators

because of growth or changing species compositions. The pattern of elevated migrator biomass did not coincide directly with the monsoon cycles; however, the timing may have evolved to use the enhanced primary and secondary production characteristic of the SWM. Reproduction in myctophids in the Gulf of Oman occurs during late winter-early spring, and with a growth rate in which the fish mature in seven months. It is plausible that enhanced migrator biomass observed in the summer (SWM) may have resulted from reproduction and growth earlier in the year (e.g., Gjøsæter, 1981, 1984; Gjøsæter and Tilseth, 1983, 1988; Prosch, 1991). Myctophids experience maximum growth during the time zooplankton biomass is highest in the shelf break area of the northern Arabian Sea. Our observed seasonal pattern was not consistent with a previous study of myctophid biomass, conducted using both net trawls and acoustic estimates, where greater biomass was observed during the spring than during the summer (Gjøsæter, 1981). This apparent discrepancy may be due to inherent patchiness of the fish populations, potential interannual variations, or the possibility that myctophid biomass is largest in slope waters (GLOBEC, 1993). Another source of inconsistency between the two studies is that the 1975 sampling (Gjøsæter, 1981) took place only between August and November, whereas our study covered a complete annual cycle. Peak abundance and largest individual size of the strongly migrating swimming crab, *Charybdis smithii* (Van Couwelaar et al., 1997), and elevated abundances of decapods (Mincks et al., 2000), were observed during the SWM, which probably contributed to our high night biomass (migrator plus zooplankton) estimates during the SWM.

#### 4.3. Predation pressure

Predation pressure was greater offshore of the Findlater Jet than inshore of the Jet or in the central Arabian Sea. This suggests that predation, and transformation of zooplankton carbon into nekton carbon, was greater in the offshore region. Hence, proportionally more zooplankton carbon would remain unconsumed inshore than offshore.

Potential predators of zooplankton that would be included in ADCP biomass estimates include myctophid fish, decapod shrimp, and pelagic crabs (e.g., Kinzer et al., 1993; Van Couwelaar, 1997; Luo et al., 2000; Mincks et al., 2000). Van Couwelaar (1997) found that the biomass of mesopelagic fish was greatest in the southern Red Sea and the Gulf of Aden during the NEM, but in the Arabian Sea off Somalia, the peak occurred during the SWM. The NEM peak in biomass in the southern Red Sea and Gulf of Aden coincided with peak primary production and zooplankton biomass; similarly the peak in biomass of mesopelagic fish off Oman occurs in the SWM at the time of highest primary and secondary production. Off Oman, the pelagic crab *Charybdis smithii* fed near the surface primarily on fish and large crustaceans (euphausiids/decapods), although some feeding on copepods may have occurred (Mincks et al., 2000).

#### 4.4. Diel vertical migration

Diel vertical migration was a consistent feature throughout the year, although the strength and coherence of the migration varied. The strength of diel vertical migration depends on the composition of the migrator community, stronger or weaker environmental cues such as light, or a combination of both. During 1995, the SWM was characterized by cloudier weather relative to other seasons (Weller et al., 1998), which may have resulted in the weaker diel vertical migration observed during that period. Weak diel vertical migration also was observed for the SWM for zooplankton alone (from 150  $\mu\text{m}$  mesh net sampling; Smith et al., 1998b). The Arabian Sea is characterized by the presence of a broad and persistent oxygen minimum zone, located below  $\sim 100\text{--}150\text{ m}$  (e.g., Morrison et al., 1999). Despite the presence of the oxygen minimum zone, migrator biomass was found within the oxygen minimum zone during daytime for all periods sampled. Clearly, the myctophids comprising the migrator biomass must have evolved adaptations to permit survival in the low-oxygen environment. The pelagic crabs (*C. smithii*), on the other hand, were found just above the oxygen minimum zone (Gjøsæter, 1981;

Kinzer et al., 1993; Van Couwelaar et al., 1997). The vertical migration velocities (150–450 m/h for downward migration and 100–250 m/h for upward migration) seen in our study are similar to migration velocities reported previously for myctophids (e.g., Gjøsaeter, 1984; Luo et al., 2000). Our migration velocities generally exceeded those reported for zooplankton in field and laboratory studies (Enright, 1977; Roe et al., 1984; Wiebe et al., 1992; references in Luo et al., 2000), supporting the assumption that myctophid fish dominated the vertically migrating backscatter intensity from the ADCP. Downward migration velocities at sunrise exceeded upward migration velocities at sunset, a pattern that also was reported for myctophid fish by Gjøsaeter (1984). The timing of vertical migrations generally preceded the times of sunrise and sunset, as has been observed in previous studies utilizing both nets and acoustic instruments (Forward, 1988; Ashjian et al., 1998; Luo et al., 2000). The relatively later downward migrations seen during the SWM and Intermonsoon periods may have resulted from different proportions of migrator types (myctophids, crabs) or different species with different migration behaviors being present.

#### 4.5. Integration with other US JGOFS studies

The physical response of the northern Arabian Sea to the Findlater Jet during the SWM has been shown to include an eddy field inshore of ~600 km (Flagg and Kim, 1998; Lee et al., 2000). Within our study area, there was a large and persistent eddy (Flagg and Kim, 1998; Manghnani et al., 1998; Dickey et al., 1998; Brink et al., 1998; Lee et al., 2000) that carried upwelled water and the included biological populations from the coastal area into the interior of the Arabian Sea. In terms of plant pigments, the offshore extent of this eddy was observed at station S8 during the SWM (Latasa and Bidigare, 1998). Dinoflagellate species at this station also were found at station S2 and are considered to be a post-diatom stage in the succession of species in the upwelling area (Garrison et al., 2000). In terms of zooplankton biomass, the eddy was essentially undetectable,

although zooplankton biomass was slightly higher at station S8 in the SWM (Fig. 3). However, at the adjacent station S7, which clustered closely with S8 (Latasa and Bidigare, 1998; S8 was not sampled with nets), the species present at the surface, *Calanoides carinatus* late subadult and adult stages, was characteristic of the upwelling area (Lane et al., 1998). Although the zooplankton biomass connection between the coast and offshore was weak, fauna from the upwelling area were present offshore and their age-structure suggests transport from the coastal upwelling area. That is, transport offshore in the eddy was observed as a succession in the phytoplankton community and maturation of the zooplankton community.

Many JGOFS biological studies focused upon the seasonal responses of the microbial loop and primary productivity of the northern Arabian Sea. These studies revealed that growth and grazing in the microbial loop were generally balanced except nearshore during the SWM (Landry et al., 1998), that picoeukaryotic algae (Campbell et al., 1998) and diatoms (Garrison et al., 2000) dominated the community nearshore in the SWM, and that *Prochlorococcus* was dominant everywhere during the SI (Campbell et al., 1998). The distribution and abundance of zooplankton are completely consistent with these findings. When *Prochlorococcus* dominated the study area (April), zooplankton biomass was low (<4 g dry weight/m<sup>2</sup>; Fig. 3) everywhere from the coast to 1000 km offshore. When diatoms were abundant in the upwelling area, zooplankton biomass reached 9 g dry weight/m<sup>2</sup> at the time when the microbial loop was most unbalanced.

#### 4.6. Significance

The intensive, year-long US JGOFS study demonstrated clearly that the dominant annual signal in upper-ocean physics and biology in the Arabian Sea results from the response to atmospheric forcing during the SWM. The strength of this monsoonal forcing over the Arabian Sea has undergone climatic cycles (Murray and Prell, 1992), from weak forcing during glaciation to strong forcing during interglacial periods, as

reflected in the Arabian Sea sediment records (Luther et al., 1990; Prell et al., 1990). Sediment records show that variability associated with monsoonal strength impacts productivity in the upper mixed layer (UML) of the Arabian Sea (Murray and Prell, 1992) and the spatial extent of the upwelling area off Oman (Prell, 1984; Luther et al., 1990). Paleooceanographic data and models (Prell, 1984; Prell et al., 1990; Luther et al., 1990), earlier studies of the nearshore waters of Oman (Smith and Bottero, 1977; Elliott and Savidge, 1990), and advanced very high resolution radiometer (AVHRR) data (Smith et al., 1998b) all demonstrate the prominent upwelling signal of the northern Arabian Sea during the SWM season. Recent studies of interannual variability in the strength of monsoonal forcing in the northwestern Indian Ocean have proposed both a regional mechanism (Webster et al., 1999; Saji et al., 1999) and a global mechanism linked to El Niño Southern Oscillation (ENSO) in the Pacific Ocean (Chambers et al., 1999; Kumar et al., 1999). In either case, the Arabian Sea is a region sensitive to changing global climate through changes in monsoonal forcing on the UML (Smith et al., 1991, 1998a; Codispoti et al., 1992; Molnar et al., 1993; Lee et al., 2000; Morrison et al., 1999). This dramatic and predictable enhancement of upper-ocean productivity may have contributed significantly to the evolution of plankton community structure and succession and has important consequences to the annual flux of carbon to the deep sea.

### Acknowledgements

We are grateful to our collaborators in the Arabian Sea project without whom this work would not have been possible. Special thanks to Y. Shi and M. Dunn (BNL) and A. Mariano, R. Kovach, and E. Ryan (RSMAS) for their assistance during data analysis and to P. Lane (RSMAS) for his many contributions. The assistance of the captain and crew of the R/V *Thomas Thompson* is gratefully acknowledged. This work was sponsored by National Science Foundation Grants #OCE9310577 and #OCE9310599 to S. L.

Smith and #OCE9310577 to C.N. Flagg and Office of Naval Research Grants #N000149510042 to S. L. Smith and #N0001494F0070 to C.N. Flagg. This is contribution number 10537 from the Woods Hole Oceanographic Institution and contribution number 704 from the US JGOFS program.

### References

- Ahlstrom, E.H., Thraillkill, T.R., 1963. Plankton volume loss with time of preservation. *CalCOFI Report* 9, 57–73.
- Ashjian, C.J., Smith, S.L., Flagg, C.N., Mariano, A.J., Behrens, W.J., Lane, P.V.Z., 1994. The influence of a Gulf Stream meander on the distribution of zooplankton biomass in the Slope Water, the Gulf Stream, and the Sargasso Sea, described using a shipboard acoustic Doppler current profiler. *Deep-Sea Research I* 41, 23–50.
- Ashjian, C.J., Smith, S.L., Flagg, C.N., Wilson, C., 1998. Patterns and occurrence of diel vertical migration of zooplankton in the Mid-Atlantic Bight measured by the acoustic Doppler current profiler. *Continental Shelf Research* 18, 831–858.
- Baars, M.A., Oosterhuis, S., 1997. Zooplankton biomass in the upper 200 m in and outside the seasonal upwelling areas of the western Arabian Sea. In: Pierrot-Bults, A.C., van der Spoel, S. (Eds.), *Pelagic Biogeography ICoPBII. Proceedings of the Second International Conference. IOC/UNESCO, Paris*, pp. 39–52.
- Banse, K., 1987. Seasonality of phytoplankton chlorophyll in the central and northern Arabian Sea. *Deep-Sea Research* 34, 713–723.
- Barber, R.T., Marra, J., Bidigare, R.C., Codispoti, L.A., Halpern, D., Johnson, Z., Latasa, M., Goericke, R., Smith, S.L., 2001. Primary productivity and its regulation in the Arabian Sea during 1995. *Deep-Sea Research II* 48, 1127–1172.
- Batchelder, H.P., Van Keuren, J.R., Vaillancourt, R., Swift, E., 1995. Spatial and temporal distributions of acoustically estimated zooplankton biomass near the Marine Light-Mixed Layers station (59°20'N, 21°00'W) in the North Atlantic in May 1991. *Journal of Geophysical Research* 100, 6549–6563.
- Boyd, C.M., Smith, S.L., 1983. Plankton, upwelling and coastally trapped waves off Peru. *Deep-Sea Research I* 30, 723–742.
- Brink, K., Arnone, R., Coble, P., Flagg, C., Jones, B., Kindle, J., Lee, C., Phinney, D., Wood, M., Yentsch, C., Young, D., 1998. Monsoons boost biological productivity in the Arabian Sea. *EOS* 79, 165–169.
- Brock, J.C., McClain, C.R., 1992. Interannual variability in phytoplankton blooms observed in the northwestern

- Arabian Sea during the southwest monsoon. *Journal of Geophysical Research* 97, 733–750.
- Brock, J.C., McClain, C.R., Luther, M.E., Hay, W.W., 1991. The phytoplankton bloom in the northwestern Arabian Sea during the southwest monsoon of 1979. *Journal of Geophysical Research* 96, 20632–20642.
- Brock, J.C., McClain, C.R., Hay, W.W., 1992. Southwest monsoon hydrographic climatology for the northwestern Arabian Sea. *Journal of Geophysical Research* 97, 9455–9465.
- Brown, O.B., Bruce, J.G., Evans, R.H., 1980. Evolution of sea surface temperature in the Somali Basin during the Southwest Monsoon of 1979. *Science* 209, 595–597.
- Buchholz, F., Buchholz, C., Reppin, J., Fischer, J., 1995. Diel vertical migrations of *Meganycitiphanes norvegica* in the Kattegat: comparison of net catches and measurements with acoustic doppler current profilers. *Helgolander Meeresuntersuchungen* 49, 849–866.
- Campbell, L., Landry, M., Constantinou, J., Nolla, H., Brown, S., Liu, H., Caron, D., 1998. Response of microbial community structure to environmental forcing in the Arabian Sea. *Deep-Sea Research II* 45, 2301–2326.
- Caron, D.A., Dennett, M.R., 1999. Phytoplankton growth and mortality during the 1005 Northeast Monsoon and Spring Intermonsoon in the Arabian Sea. *Deep-Sea Research II* 46, 1665–1690.
- Chambers, D., Tapley, B., Stewart, R., 1999. Anomalous warming in the Indian Ocean coincident with El Niño. *Journal of Geophysical Research* 104 (C2), 3035–3047.
- Codispoti, L., Elkins, J., Yoshinari, T., Friederich, G., Sakamoto, C., Packard, T., 1992. On the nitrous oxide flux from productive regions that contain low oxygen waters. In: Desai, B.N. (Ed.), *Oceanography of the Indian Ocean*. Oxford & IBH Publishing Co., New Delhi, pp. 271–284.
- Currie, R.I., Fisher, A.E., Hargreaves, P.M., 1973. Arabian Sea upwelling. In: Zeitschel, B. (Ed.), *The Biology of the Indian Ocean*. Springer, NY, pp. 475–486.
- Dalpadado, P., Gjøsaeter, J., 1988. Feeding ecology of the lanternfish *Benthoosema pterotum* from the Indian Ocean. *Marine Biology* 99, 555–567.
- Dickey, T., Marra, J., Sigurdson, D., Weller, R., Kinkade, C., Zedler, S., Wiggert, J., Langdon, C., 1998. Seasonal variability of bio-optical and physical properties in the Arabian Sea: October 1994–October 1995. *Deep-Sea Research II* 45, 2001–2026.
- Elliott, A.J., Savidge, G., 1990. Some features of the upwelling off Oman. *Journal of Marine Research* 48, 319–333.
- Enright, J.T., 1977. Copepods in a hurry: sustained high-speed upward migration. *Limnology and Oceanography* 22, 118–125.
- Estrada, M., 1974. Photosynthetic pigments and productivity in the upwelling region off northwest Africa. *Tethys* 6, 247–260.
- Fischer, J., Visbeck, M., 1993. Seasonal variation of the daily zooplankton migration in the Greenland Sea. *Deep-Sea Research I* 40, 1547–1557.
- Flagg, C.N., Smith, S.L., 1989. On the use of the acoustic Doppler current profiler to measure zooplankton abundance. *Deep-Sea Research* 36, 455–474.
- Flagg, C., Kim, H.-S., 1998. Upper ocean currents in the northern Arabian Sea from shipboard ADCP measurements collected during the 1994–1996 US JGOFS and ONR programs. *Deep-Sea Research II* 45, 1917–1960.
- Flagg, C.N., Wirick, C.D., Smith, S.L., 1994. The interaction of phytoplankton, zooplankton, and currents from 15 months of continuous data in the Mid-Atlantic Bight. *Deep-Sea Research II* 41, 411–435.
- Forward, R.B., Jr, 1988. Diel vertical migration: Zooplankton photobiology and behaviour. *Oceanography and Marine Biology Annual Review* 26, 361–393.
- Gardner, W.D., Gundersen, J.S., Richardson, M.J., Walsh, I.D., 1999. The role of seasonal and diel changes in mixed-layer depth on carbon and chlorophyll distributions in the Arabian Sea. *Deep-Sea Research II* 46, 1833–1859.
- Garrison, D., Gowing, M., Hughes, M., Campbell, L., Caron, D., Dennett, M., Shalapyonok, S., Olson, R., Landry, M., Brown, S., Liu, H., Azam, F., Steward, G., Ducklow, H., Smith, D., 2000. Microbial food web structure in the Arabian Sea: a US JGOFS study. *Deep-Sea Research II* 47, 1387–1422.
- Gjøsaeter, J., 1981. Abundance and production of lanternfish (Myctophidae) in the western and northern Arabian Sea. *Fiskeridirektoratets Skrifter Serie Havundersøkelser* 17, 215–251.
- Gjøsaeter, J., 1984. Mesopelagic fish, a large potential resource in the Arabian Sea. *Deep-Sea Research I* 31, 1019–1035.
- Gjøsaeter, J., Tilseth, S., 1983. Survey of mesopelagic fish resources in the Gulf of Oman. *Institute of Marine Research, University of Bergen, Bergen, Norway*, 30pp.
- Gjøsaeter, J., Tilseth, S., 1988. Spawning behaviour, egg and larval development of the myctophid fish *Benthoosema pterotum*. *Marine Biology* 98, 1–6.
- GLOBEC, 1993. Implementation Plan and Workshop Report for US GLOBEC Studies in the Arabian Sea. *US Global Ocean Ecosystems Dynamics Report Number 9*, 105pp.
- Gunderson, J.S., Gardner, W.D., Richardson, M.J., Walsh, I.D., 1998. Effects of monsoons on the seasonal and spatial distributions of POC and chlorophyll in the Arabian Sea. *Deep-Sea Research II* 45, 2103–2132.
- Herring, P.J., Fasham, M.J.R., Weeks, A.R., Hemmings, J.C.P., Roe, H.S.R., Pugh, P.R., Holley, S., Crisp, N.A., Angel, M.V., 1998. Across-slope relations between the biological populations, the euphotic zone, and the oxygen minimum layer off the coast of Oman during the southwest monsoon (August, 1994). *Progress in Oceanography* 41, 69–109.
- Heywood, K.J., 1996. Diel vertical migration of zooplankton in the Northeast Atlantic. *Journal of Plankton Research* 18, 163–184.
- Heywood, K.J., Scrope-Howe, S., Barton, E.D., 1991. Estimation of zooplankton abundance from shipborne ADCP backscatter. *Deep-Sea Research I* 38, 667–691.

- Holliday, D.V., Pieper, R.E., 1995. Bioacoustical oceanography at high frequencies. *ICES Journal of Marine Science* 52, 279–296.
- Kinzer, J., Schulz, K., 1991. Distribution and diet of myctophids in the NE Arabian Sea. Proceedings of the Symposium on the Indian Ocean. National Institute of Oceanography, Goa, India (Abstract).
- Kinzer, J., Böttger-Schnak, R., Schulz, K., 1993. Aspects of the horizontal distribution and diet of myctophid fishes in the Arabian Sea with reference to the deep water oxygen deficiency. *Deep-Sea Research II* 40, 783–800.
- Kumar, K., Kleeman, R., Cane, M., Rajagopalan, B., 1999. Epochal changes in Indian monsoon-ENSO precursors. *Geophysical Research Letters* 26, 75–78.
- Landry, M., Brown, S., Campbell, L., Constantinou, J., Liu, H., 1998. Spatial patterns in phytoplankton growth and microzooplankton grazing in the Arabian Sea during monsoon forcing. *Deep-Sea Research II* 45, 2353–2368.
- Lane, P., Smith, S., Zaragoza, J., Prusova, I., Roman, M., 1998. US JGOFS Technical Report: Copepod taxonomy, abundance and biomass in the upper 300 meters of the Arabian Sea during the Southwest Monsoon (August/September) of 1995. RSMAS Technical Report number 98-007. The Rosenstiel School, University of Miami, Miami, FL, 409pp.
- Latasa, M., Bidigare, R., 1998. A comparison of phytoplankton populations of the Arabian Sea during the Spring Intermonsoon and Southwest Monsoon of 1995 as described by HPLC-analyzed pigments. *Deep-Sea Research II* 45, 2133–2170.
- Lee, C.M., Jones, B.H., Brink, K.H., Fischer, A.S., 2000. The upper-ocean response to monsoonal forcing in the Arabian Sea: seasonal and spatial variability. *Deep-Sea Research II* 47, 1177–1226.
- Luo, J., Ortner, P.B., Forcucci, D., Cummings, S.R., 2000. Diel vertical migration of zooplankton and mesopelagic fish in the Arabian Sea. *Deep-Sea Research II* 47, 1451–1473.
- Luther, M., O'Brien, J., Prell, W., 1990. Variability in upwelling fields in the northwestern Indian Ocean I. Model experiments for the past 18,000 years. *Paleoceanography* 5, 433–445.
- Lutjeharms, J.R.E., Stockton, P.L., 1987. Kinematics of the upwelling front off southern Africa. *South African Journal of Marine Science* 5, 35–49.
- Lyons, M.G., Smith, P.E., Moser, H.G., 1994. Comparison of cross-shelf trends in acoustic Doppler current profiler amplitude and zooplankton displacement volume in southern California. *CalCOFI Report* 35, 240–245.
- Madhupratap, M., Kumar, S.P., Bhattathiri, P.M.A., Kumar, M.D., Raghukumar, S., Nair, K.K.C., Ramaiah, N., 1996a. Mechanism of the biological response to winter cooling in the Arabian Sea. *Nature* 384, 549–552.
- Madhupratap, M., Gopalakrishnan, T.C., Haridas, P., Nair, K.K.C., Aravindakshan, P.N., Padmavati, G., Paul, S., 1996b. Lack of seasonal and geographic variation in mesozooplankton biomass in the Arabian Sea and its structure in the mixed layer. *Current Science* 71, 863–868.
- Manghnani, V., Morrison, J., Hopkins, T., Böhm, E., 1998. Advection of upwelled waters in the form of plumes off Oman during the Southwest Monsoon. *Deep-Sea Research II* 45, 2027–2052.
- Mariano, A.J., Brown, O.B., 1992. Efficient objective analysis of dynamically heterogeneous and nonstationary fields via the parameter matrix. *Deep Sea Research I* 39, 1255–1271.
- Marra, J., Dickey, T.D., Ho, C., Kinkade, C.S., Sigurdson, D.E., Weller, R.A., Barber, R.T., 1998. Variability in primary production as observed from moored sensors in the central Arabian Sea in 1995. *Deep-Sea Research II* 45, 2253–2268.
- Matthew, K., Naomi, T., Antony, G., Vincent, D., Anikumar, R., Solomon, K., 1990. Studies on zooplankton biomass and secondary and tertiary production of the EEZ of India. Proceedings of the First Workshop on Scientific Results of FORV *Sagar Sampada*, pp. 59–60.
- Mincks, S.L., Bollens, S.M., Madin, L.P., Horgan, E., Butler, M., Kremer, P.M., Craddock, J.E., 2000. Distribution, abundance, and feeding ecology of decapods in the Arabian Sea, with implications for vertical flux. *Deep-Sea Research II* 47, 1475–1516.
- Molnar, P., England, P., Martinod, J., 1993. Mantle dynamics, uplift of the Tibetan Plateau, and the Indian Monsoon. *Reviews of Geophysics* 31 (4), 357–396.
- Morrison, J.M., Codispoti, L.A., Smith, S.L., Wishner, K., Flagg, C., Gardner, W.D., Gaurin, S., Naqvi, S.W.A., Manghnani, V., Prosperie, L., Gundersen, J.S., 1999. The oxygen minimum zone in the Arabian Sea during 1995. *Deep-Sea Research II* 46, 1903–1932.
- Morrison, J.M., Codispoti, L.A., Gaurin, S., Jones, B., Manghnani, V., Zheng, Z., 1998. Seasonal variations of hydrographic and nutrient fields during the US JGOFS Arabian Sea Process Study. *Deep-Sea Research II* 45, 2053–2102.
- Murray, D., Prell, W., 1992. Late Pliocene and Pleistocene climatic oscillations and monsoon upwelling recorded in sediments from the Owen Ridge, Northwestern Arabian Sea. In: Summerhayes, C., Prell, W., Emeis, K. (Eds.), *Upwelling Systems: Evolution since the early Miocene*. Geological Society Special Publication No. 64, pp. 301–321.
- Nafpaktitis, B.G., 1978. Systematics and distribution of lanternfishes of the genera *Lobianchia* and *Diaphus* in the Indian Ocean. *Bulletin of the Los Angeles County Museum* 30, 1–92.
- Pearre Jr., S., 1979. Problems of detection and interpretation of vertical migration. *Journal of Plankton Research* 1, 29–44.
- Pieper, R.E., McGehee, D.E., Greenlaw, C.F., Holiday, D.V., 2001. Acoustically measured seasonal patterns of zooplankton in the Arabian Sea. *Deep-Sea Research II* 48, 1325–1343.

- Plueddemann, A.J., Pinkel, R., 1989. Characterization of the patterns of diel migration using a Doppler sonar. *Deep-Sea Research I* 36, 509–530.
- Prell, W., 1984. Variation in monsoonal upwelling: a response to changing solar radiation. In: Hansen, J., Takahashi, T., (Eds.), *Climate Processes and Climate Sensitivity*. American Geophysical Union, Geophysical Monograph Series 29, pp. 48–57.
- Prell, W., Marvil, R., Luther, M., 1990. Variability in upwelling fields in the northwestern Indian Ocean 2. Data-model comparison at 9000 years BP. *Paleoceanography* 5, 447–457.
- Prosch, R.M., 1991. Reproductive biology and spawning of the myctophid *Lampanyctodes Hectoris* and the sternoptychid *Maurollicus muelleri* in the southern Benguela ecosystem. *South African Journal Marine Science* 10, 241–252.
- Qasim, S., 1977. Contribution of zooplankton in the food chains of some warm water environments. *Proceedings of the Symposium on Warm Water Zooplankton*, National Institute of Oceanography, Goa, pp. 700–708.
- RD Instruments, 1990. Calculating absolute backscatter. RD Instruments Technical Bulletin ADCP-90-04, 24pp.
- Roe, H.S.J., Griffiths, G., 1993. Biological information from an acoustic Doppler current profiler. *Marine Biology* 115, 339–346.
- Roe, H.S., Angel, M.V., Badcock, J., Domanski, P., James, P.T., Pugh, P.R., Thurston, M.H., 1984. The diel migrations and distributions within a mesopelagic community in the northeast Atlantic. *Progress in Oceanography* 13, 245–511.
- Ropke, A., Nellen, W., Piatkowski, U., 1993. A comparative study in the influence of the pycnocline on the vertical distribution of fish larvae and cephalopod paralarvae in three ecologically different areas of the Arabian Sea. *Deep-Sea Research II* 40, 801–821.
- Saji, N., Goswami, B., Vinayachandran, P., Yamagata, T., 1999. A dipole mode in the tropical Indian Ocean. *Nature* 401, 360–363.
- SAS Institute Inc., 1985. *SAS Users Guide; Statistics*. Version 5 edition. SAS Institute Inc., Cary, NC, 956pp.
- Schott, F., Swallow, J.C., Fieux, M., 1990. The Somali Current at the equator: annual cycle of currents and transports in the upper 1000 m and connection to neighboring latitudes. *Deep-Sea Research I* 37, 1825–1848.
- Smith, S.L., 1982. The northwestern Indian Ocean during the monsoons of 1979: distribution, abundance, and feeding of zooplankton. *Deep-Sea Research I* 29, 1331–1353.
- Smith, S.L., 1984. Biological indications of active upwelling in the northwestern Indian Ocean in 1964 and 1979, and a comparison with Peru and northwest Africa. *Deep-Sea Research I* 31, 951–967.
- Smith, S.L., 2001. Understanding the Arabian Sea: reflections on the 1994–1996 Arabian Sea expedition. *Deep-Sea Research II* 48, 1385–1402.
- Smith, R.L., Bottero, J.S., 1977. On upwelling in the Arabian Sea. In: Angel, M. (Ed.), *A Voyage of Discovery*, Supplement to *Deep-Sea Research*. Pergamon Press, Oxford, pp. 291–304.
- Smith, S.L., Codispoti, L.A., 1980. Southwest monsoon of 1979: chemical and biological response of Somali coastal waters. *Science* 209, 596–600.
- Smith, S., Banse, K., Cochran, J., Codispoti, L., Ducklow, H., Luther, M., Olson, D., Peterson, W., Prell, W., Surgi, N., Swallow, J., Wishner, K., 1991. US JGOFS: Arabian Sea Process Study. US JGOFS Planning Report No. 13. Woods Hole Oceanographic Institution, Woods Hole, MA, 164pp.
- Smith, S.L., Pieper, R.E., Moore, M.V., Rudstam, L.G., Greene, C.H., Zamon, J.E., Flagg, C.N., Williamson, C.E., 1992. Acoustic techniques for the in situ observation of zooplankton. *Ergebnisse der Limnologie* 36, 23–43.
- Smith, S., Codispoti, L., Morrison, J., Barber, R., 1998a. The 1994–96 Arabian Sea Expedition: an integrated, interdisciplinary investigation of the response of the northwestern Indian Ocean to monsoonal forcing. *Deep-Sea Research II* 45, 1905–1915.
- Smith, S., Roman, M., Prusova, I., Wishner, K., Gowing, M., Codispoti, L.A., Barber, R., Marra, J., Flagg, C., 1998b. Seasonal response of zooplankton to monsoonal reversals in the Arabian Sea. *Deep-Sea Research II* 45, 2369–2403.
- Stanton, T.K., Chu, D., Wiebe, P.H., Clay, C.S., 1993. Average echoes from randomly oriented, random-length finite cylinders: zooplankton models. *Journal of the Acoustical Society of America* 94, 3463–3472.
- Stanton, T.K., Wiebe, P.H., Chu, D., Benfield, M., Scanlon, L., Martin, L., Eastwood, R.L., 1994. On acoustic estimates of zooplankton biomass. *ICES Journal of Marine Science* 51, 505–512.
- Van Couwelaar, M., Angel, M.V., Madin, L.P., 1997. The distribution and biology of the swimming crab *Charybdis smithii* McLeay, 1838 (Crustacea; Brachyura; Portunidae) in the NW Indian Ocean. *Deep-Sea Research II* 44, 1251–1280.
- Webster, P., Moore, A., Loschnigg, J., Leben, R., 1999. Coupled ocean-atmosphere dynamics in the Indian Ocean during 1997–98. *Nature* 401, 356–360.
- Weller, R.A., Baumgartner, M.F., Josey, S.A., Fischer, A.S., Kindle, J.C., 1998. Atmospheric forcing in the Arabian Sea during 1994–1995: observations and comparisons with climatology and models. *Deep-Sea Research II* 45, 1961–2000.
- Wiebe, P., 1988. Functional regression equations for zooplankton displacement volume, wet weight, dry weight, and carbon: a correction. *Fishery Bulletin* 86, 833–835.
- Wiebe, P.H., Greene, C.H., 1994. The use of high frequency acoustics in the study of zooplankton spatial and temporal patterns. *Polar Biology* 7, 133–157.
- Wiebe, P.H., Boyd, S., Cox, J.L., 1975. Relationships between zooplankton displacement volume, wet weight, dry weight, and carbon. *Fishery Bulletin* 73, 777–786.
- Wiebe, P.H., Burt, K.H., Boyd, S.H., Morton, A.W., 1976. A multiple opening/closing net and environmental sensing system for sampling zooplankton. *Journal of Marine Research* 34, 341–354.
- Wiebe, P.H., Copley, N.J., Boyd, S.H., 1992. Coarse-scale horizontal patchiness and vertical migration of zooplankton

- in Gulf Stream warm-core ring 82-H. *Deep-Sea Research I* 39, S247–S278.
- Wishner, K.G., Gowing, M.M., Gelfman, C., 1998. Mesozooplankton biomass in the upper 1000 m in the Arabian Sea: overall seasonal and geographic patterns, and relationship to oxygen gradients. *Deep-Sea Research II* 45, 2405–2432.
- Zar, J.H., 1984. *Biostatistical Analysis*. Prentice-Hall Inc., Englewood Cliffs, NJ 07362, 718pp.
- Zhou, M., Nordhausen, W., Huntley, M., 1994. ADCP measurements of the distribution and abundance of euphausiids near the Antarctic Peninsula in winter. *Deep-Sea Research I* 41, 1425–1455.